

Georges Matheron Lecture on
**MATHEMATICAL MORPHOLOGY IN
GEOMORPHOLOGY AND GISCI**

B.S. DAYA SAGAR

<http://www.isibang.ac.in/~bsdsagar>



Systems Science and Informatics Unit (SSIU)

**Indian Statistical Institute,
Bangalore, INDIA**

6th September 2011



INDIAN STATISTICAL INSTITUTE

Bangalore Centre

FOUNDING FATHERS OF

MATHEMATICAL MORPHOLOGY

Georges Matheron

Jean Serra



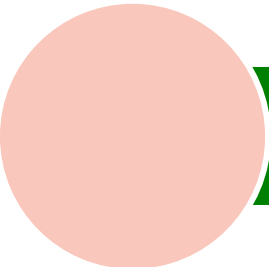
My Connection Degree



First degree separation with Jean Serra



Two-degree separation with Georges Matheron
(through SVLN Rao and Jean Serra)



SVLN Rao (v. 31, no. 2, *Mathematical Geosciences*; Associate Editor for MG 1975-77).

GEORGES MATHERON

LECTURERS



Jean Serra
2006



Wynand Kleingeld
2007



Adrian Baddeley
2008



Jean-Laurent Mallet
2009



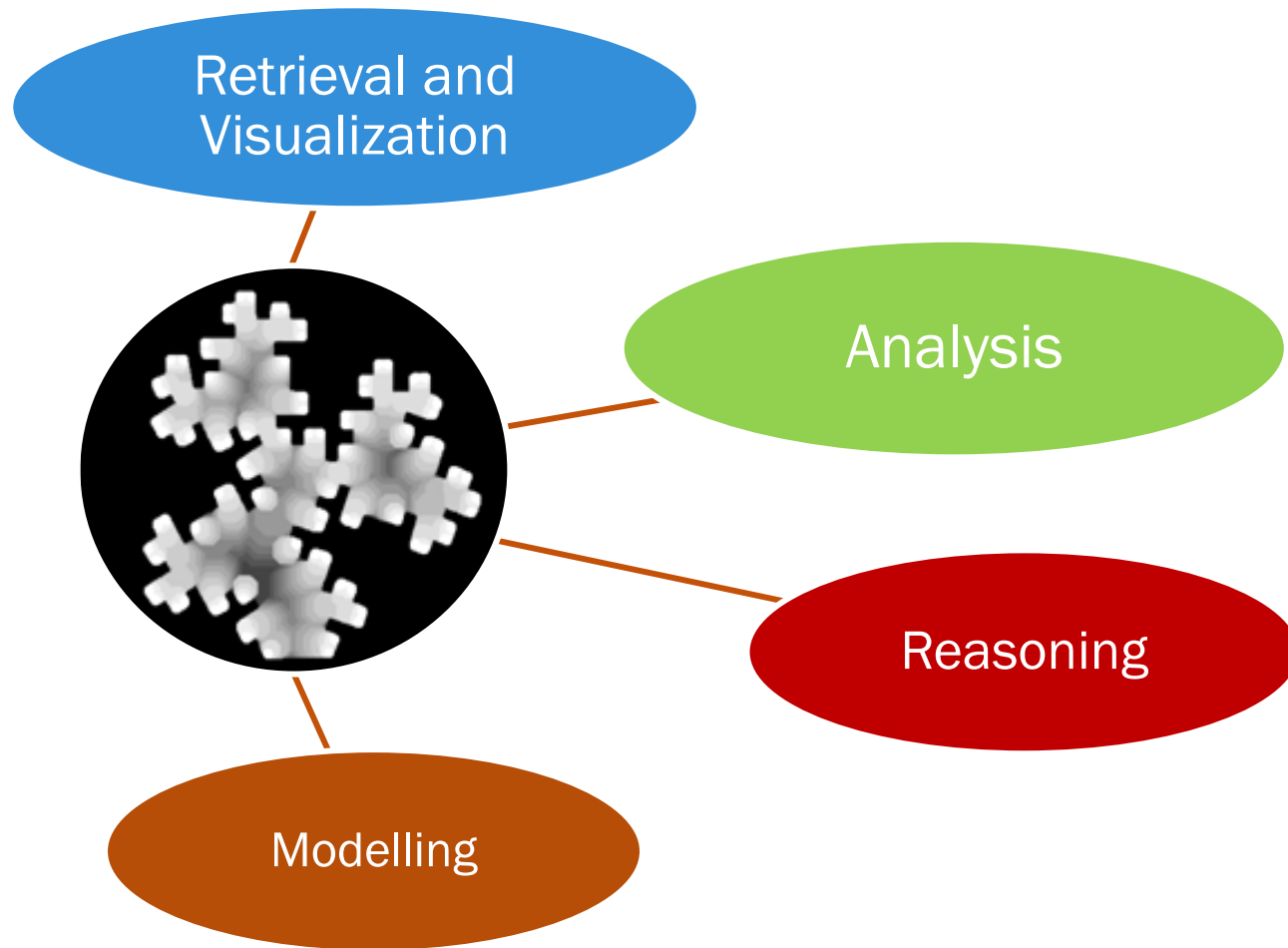
Donald A. Singer
2010

Motivation

To understand the dynamical behavior of a phenomenon or a process, development of a good **spatiotemporal model** is essential. To develop a good spatiotemporal model, well-**analyzed** and well-**reasoned information** that could be **extracted / retrieved** from spatial and/or temporal data are important ingredients.

Mathematical Morphology is one of the better choices to deal with all these key aspects mentioned.

Mathematical Morphology in Geomorphology and GISci



Outline

Basic description of Terrestrial Data

Mathematical Morphology in Geomorphology and GISci

Retrieval of Geomorphological phenomena (e.g. Networks), Analysis and quantitative characterization of Geomorphological phenomena and processes via various metrics

Spatial interpolation, Spatio-temporal modeling, spatial reasoning, spatial information visualization

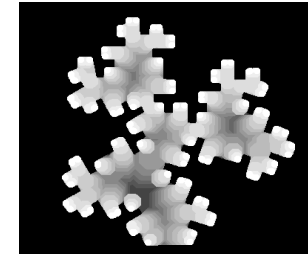
Concepts, Techniques & Tools



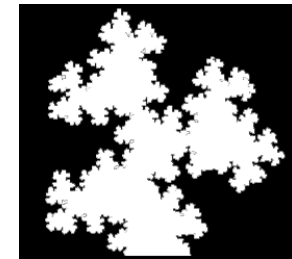
- Morphological Skeletonization
- Multiscale operations, Hierarchical segmentation
- Recursive Morphological Pruning
- Hit-or-Miss Transformation
- Morphological Thinning
- Morphological Reconstruction
- Watersheds
- Morphological shape decomposition
- Granulometries
- Hausdorff dilation (erosion) distance
- Morphological interpolation
- Directional Distances
- SKIZ and WSKIZ

Terrestrial Data : Various Representations

Functions (DEMs, Satellite Images, Microscopic Images etc)



Sets (Thresholded Elevation regions, Binary images decomposed from images)



Skeletons (Unique topological networks)



I. Mathematical Morphology

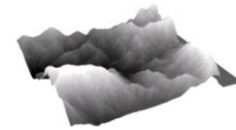
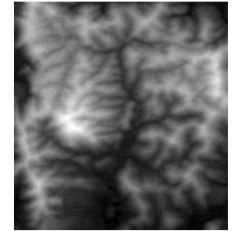
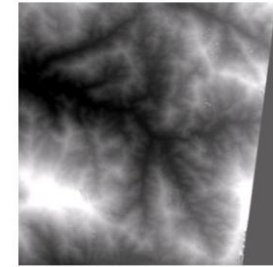
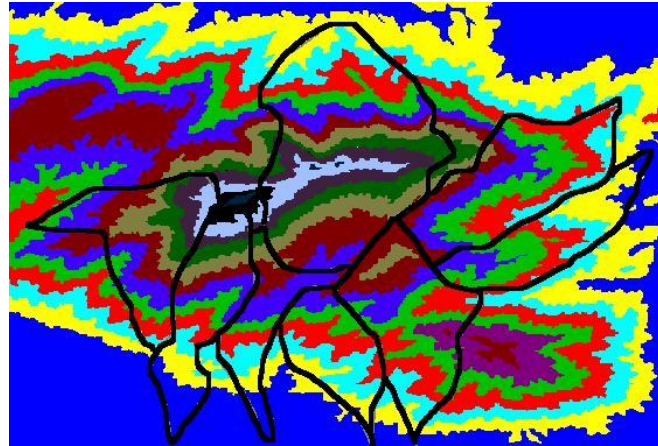
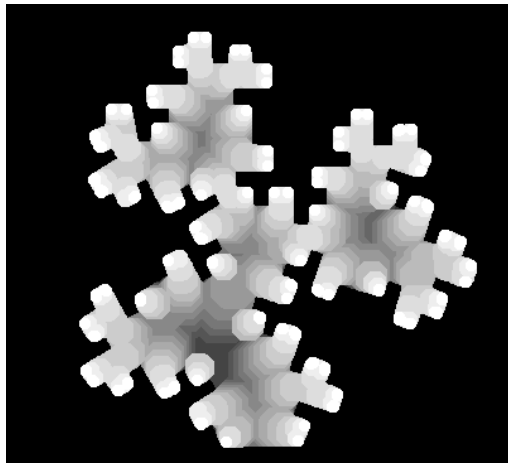


Binary Mathematical
Morphology



Grayscale Morphology

Digital Elevation Models



II.I NETWORKS EXTRACTION & THEIR PROPERTIES

12

Networks extraction and their properties :

Sub-basins delineation

- ∞ **Geomorphologic basin** is an area outlined by a topographic boundary that diverts water flow to stream networks flowing into a single outlet.
- ∞ **DEM** is an useful source for watershed and network extraction.
- ∞ **Hydrologic flow** is modelled using eight-direction pour point model (Puecker et. al., 1975).

75	73	72
73	70 →	69
74	72	71

- ∞ The two topologically significant networks, include **Channel** & **Ridge** networks.
- ∞ The paths of these extracted networks are the **crenulations** in the elevation contours.
- ∞ **Crenulations** can be isolated from DEMs by using nonlinear morphological transformations.

Network Extraction: Binary Morphology-Based

Step-1:

**Threshold
decomposition
of $f(x,y)$**

Step 2:

Skeletonization

Step 3:

**Systematic logical
union and difference to
extract network within
each spatially
distributed region and
Union of network(s)
obtained**

Equations for Network Extraction

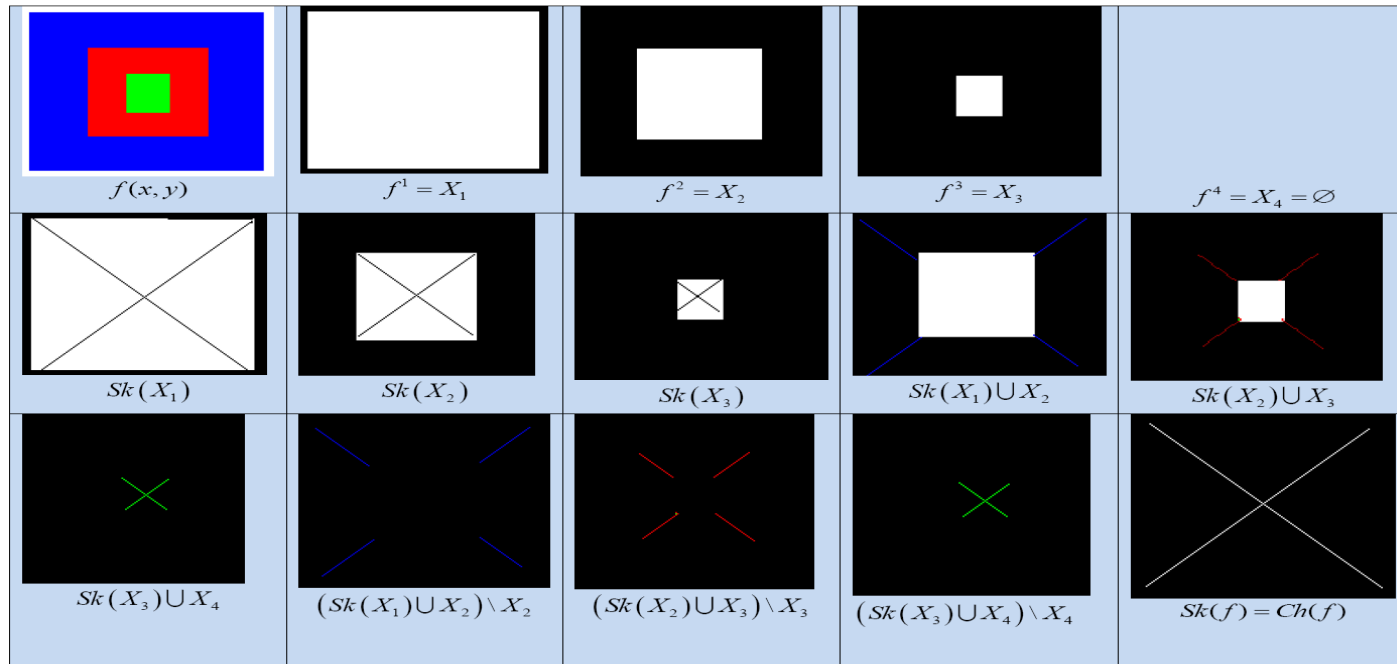
$$f^t = \begin{cases} 1 & \text{if } f(x, y) \geq t \\ 0 & \text{if } f(x, y) < t \end{cases} \quad \text{where } 0 \leq f(x, y) \leq 255$$

$$f^t = X_t; f^{t+1} = X_{t+1}; \dots; f^N = X$$

$$Sk_n(X_t) = (X_t \ominus nB) \setminus (X_t \ominus nB) \circ B \quad n = 0, 1, 2, \dots, N$$

$$Sk(X_t) = \bigcup_{n=0}^N Sk_n(X_t)$$

$$CH(f) = \bigcup_{t=1}^{255} ((Sk(X_t) \cup X_{t+1}) \setminus X_{t+1})$$



Networks extraction: Grayscale Morphology-Based

- ∞ The DEM, f is first eroded by B_n with $n=1, 2, \dots, N$, and the eroded DEM is opened by B of the smallest size. The opened version of each eroded image is subtracted from the corresponding eroded image to produce the n th level subsets of the ridge network. Union of these subsets of level $n = 0$ to N gives the ridge network for the DEM.

$$\text{RID}_n^i(f) = [(f \ominus B_n^i) \setminus \{[(f \ominus B_n^i) \ominus B_1^i] \oplus B_1^i\}]$$

$$\text{RID}(f) = \bigcup_{n=0}^N \bigcup_{i=1}^4 [\text{RID}_n^i(f)]$$

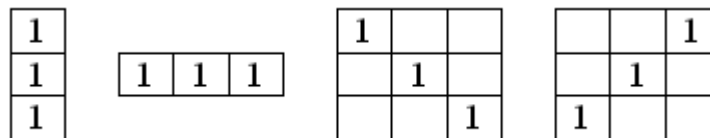
Networks extraction and their properties

- DEM, f is first dilated by B_n and the dilated f is closed by B of the smallest size. The closed version of each dilated image is subtracted from the corresponding dilated image to produce the n th level subsets of the channel network. Union of these subsets of level $n = 0$ to N gives the channel network for the DEM.

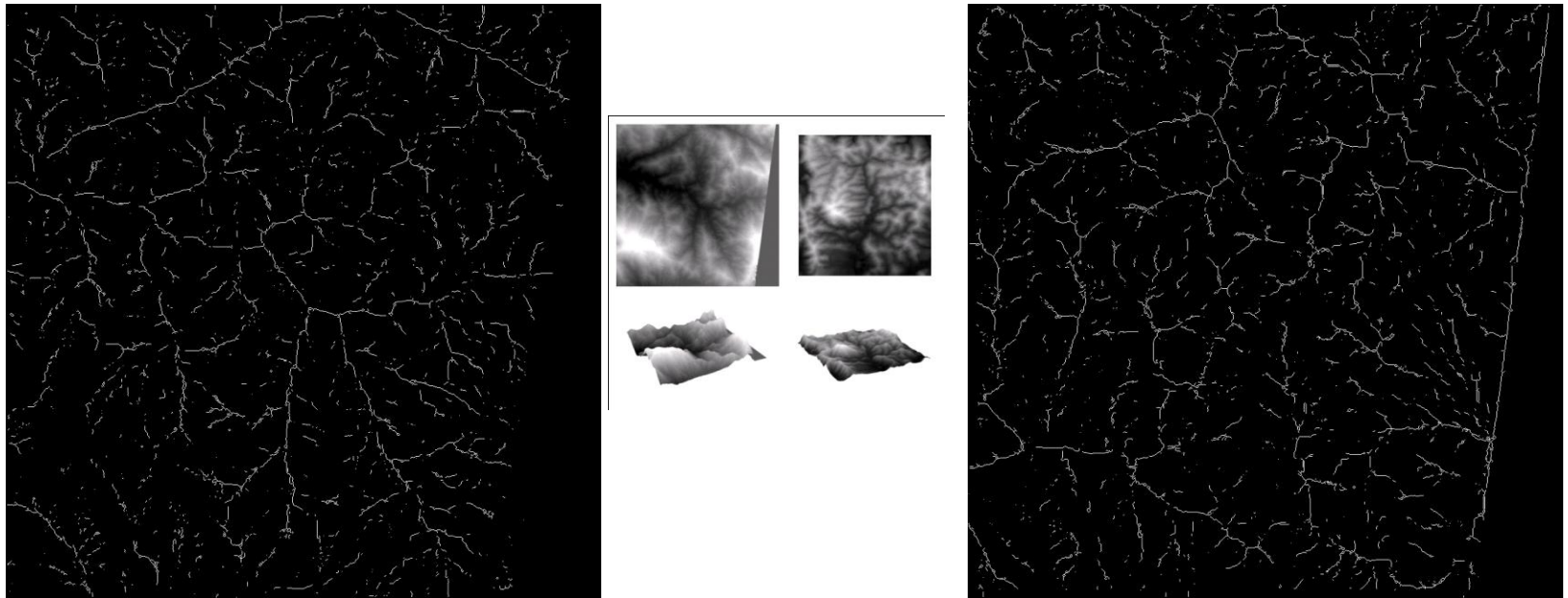
$$\text{CH}_n^i(f) = [(f \oplus B_n^i) \setminus \{[(f \oplus B_n^i) \oplus B_1^i] \ominus B_1^i\}]$$

$$\text{CH}(f) = \bigcup_{n=0}^4 \bigcup_{i=1}^N [\text{CH}_n^i(f)]$$

- 1-D structuring elements of primitive size

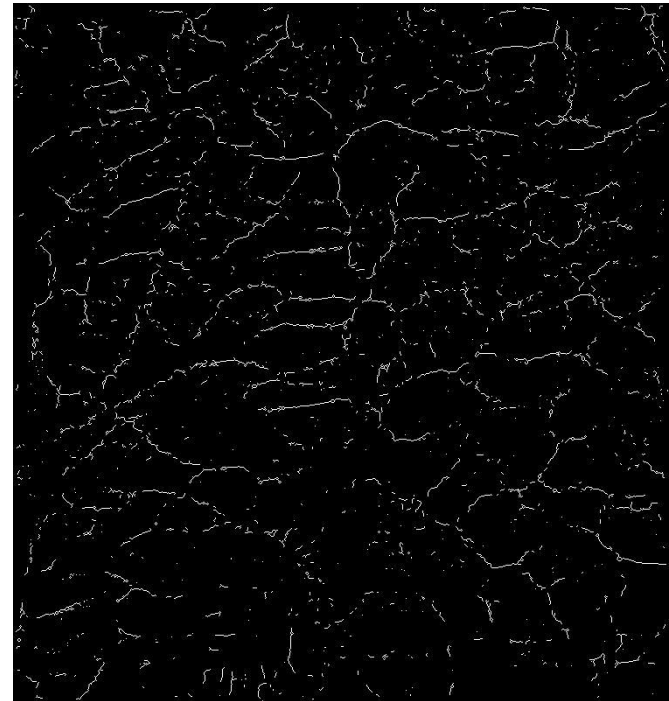
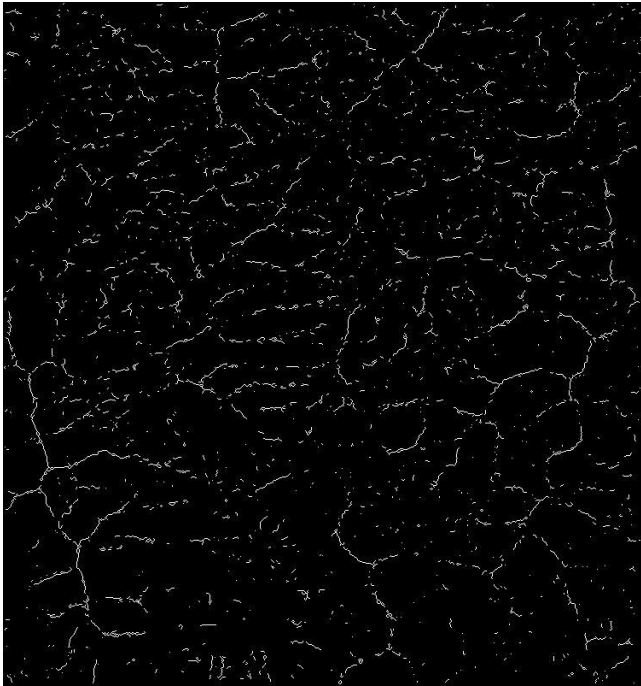


Networks extraction and their properties



(a) Ridge networks, and (b) channel networks extracted from Cameron Highlands DEM.

Networks extraction and their properties



(a) Ridge networks, and (b) channel networks extracted from Petaling DEM.

Algorithm

- ◆ Algorithm is to extract singular networks such as channel and ridge connectivity networks from DEMs.
- ◆ Sub watershed boundary in DEM is automatically generated by considering channel and ridge connectivity networks.
- ◆ Mathematical morphology transformations such as dilation, erosion, opening and closing are used in this algorithm.

∞ Step-1:

$$CH_e(M) = \epsilon_s^e(M) / \gamma_s^1(\epsilon_s^e(M))$$

$$e = 0, 1, 2, \dots, N$$

∞ Step-2:

$$CH(M) = \bigcup_{e=0}^N CH_e(M)$$

$$e = 0, 1, 2, \dots, n$$

∞ Step-3:

$$RID_e(M) = \epsilon_s^e(\{CH(M)^c\}) // \gamma_s^1(\epsilon_s^e(\{CH(M)^c\}))$$

∞ Step-4:

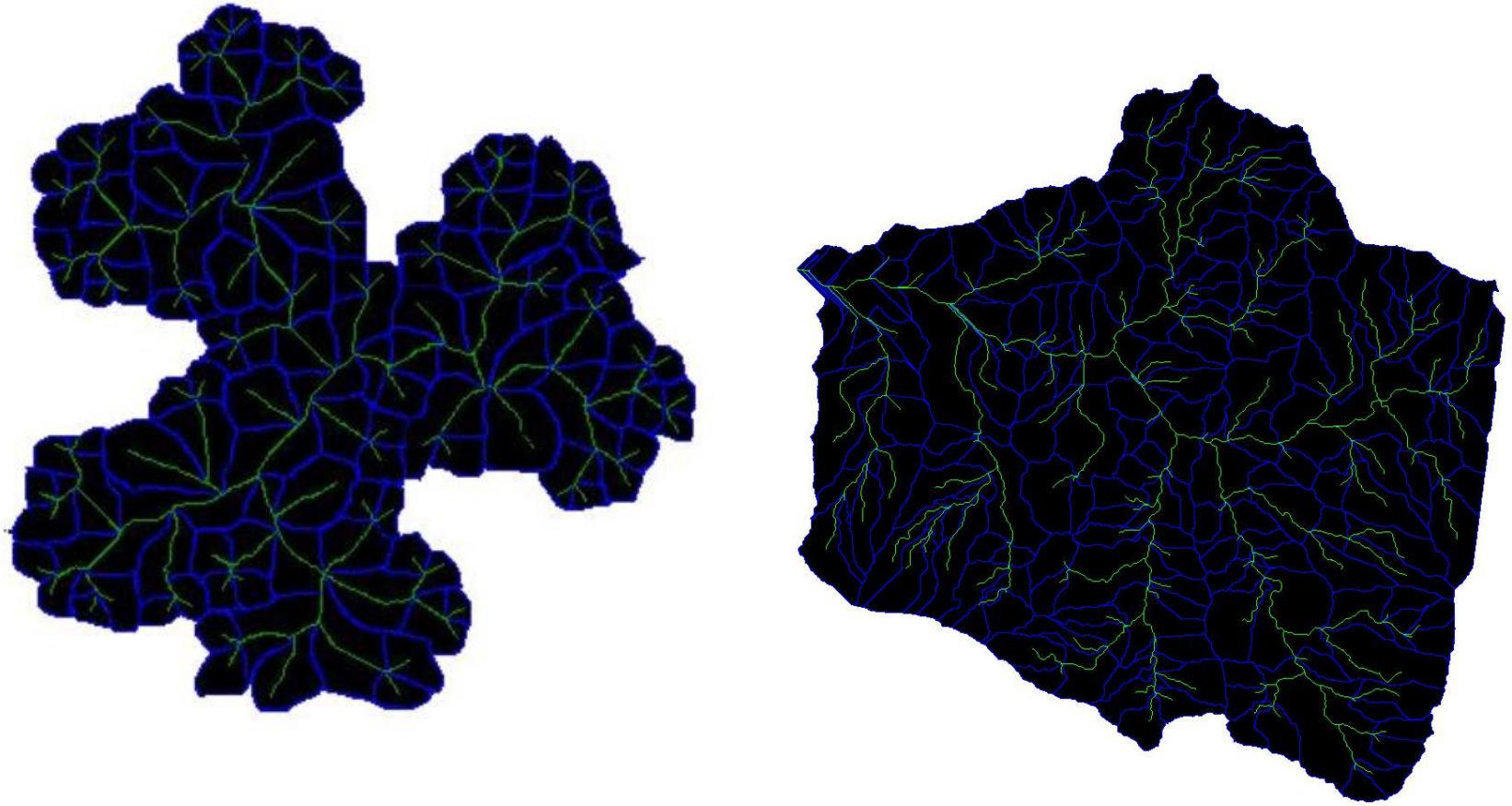
$$RID(M) = \bigcup_{e=1}^N RID_e(M)$$

$$e = 0, 1, 2, \dots, n$$

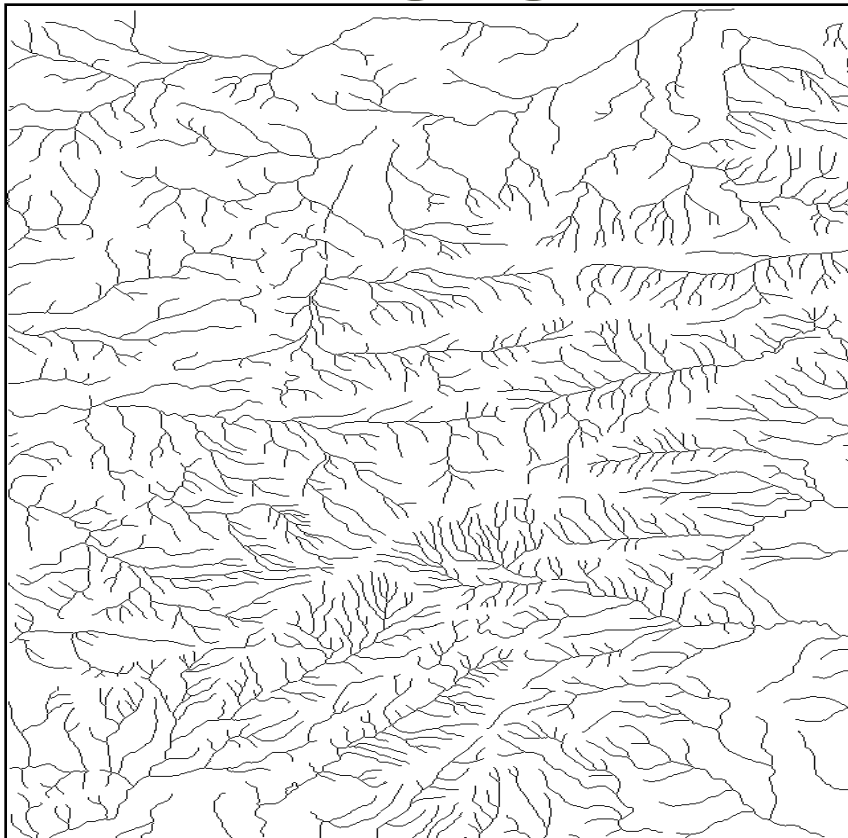
∞ Step-5:

$$CH(M) \cup RID(M)$$

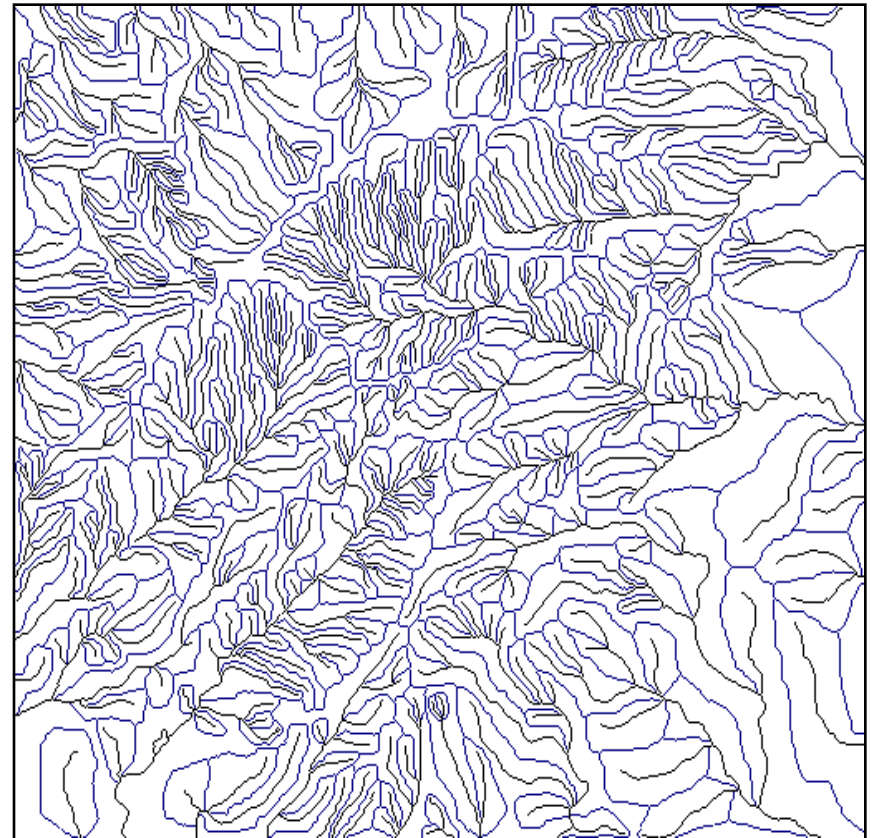
Decomposed basins and networks



Channel Network of Gunung Ledang Region



Ridge Network of Gunung Ledang Region



Networks : Binary Vs Grayscale

Binary Morphology

Binary morphology-based network extraction is:

- more stable,
- more accurate, and
- computationally expensive

Gray-scale Morphology

Grayscale-based network extraction—

- may not be accurate like binary-morphology based—
 - generates network that yields disconnections some times, but
- computationally not expensive.

II.II. Terrestrial Analysis

Scale invariance and Power-laws in networks

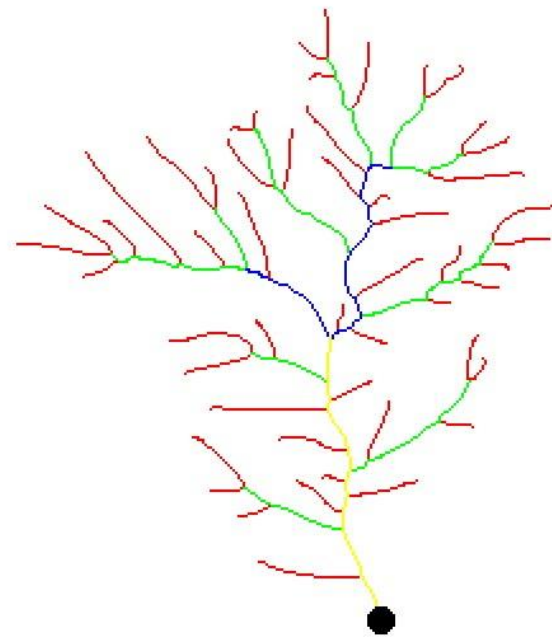
Shape-dependant power-laws

Granulometric analysis

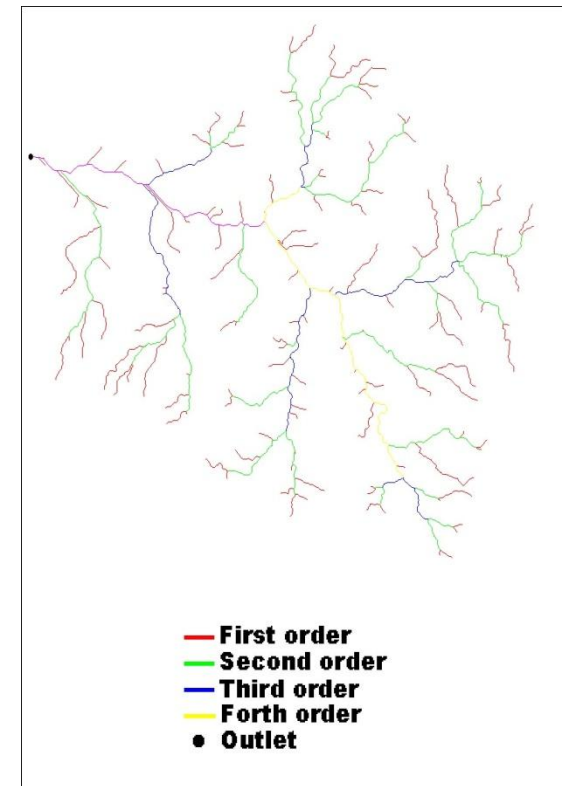
II.II.I. Scale Invariant Power-laws: Morphometry and Allometry of Networks

First step in drainage basin analyses is the classification of stream orders by Horton-Strahler's ordering system (Horton, 1945; Strahler, 1957). The order of the whole tree is defined to be the order of the root. This ordering system has been found to correlate well with important basin properties in a wide range of environments.

This figure shows a sample network classified based on Horton-Strahler's ordering system.



— **First order**
— **Second order**
— **Third order**
— **Fourth order**
● **Outlet**
Model network.



Cameron Highland channel network.

Scale Invariant Power-laws: Two Topological Quantities

- Two topological quantities bifurcation ratio (R_b) and length ratio (R_l)

$$R_b = \frac{N_i}{N_{i+1}} \qquad R_l = \frac{L_i}{L_{i-1}}$$

Networks extraction and their properties : Morphometry

- Besides these two ratios, the universal similarity of stream network can be shown through Hack's law and Hurst's law as follows:

- Hack's Law: $L_{mc} \propto A^h$

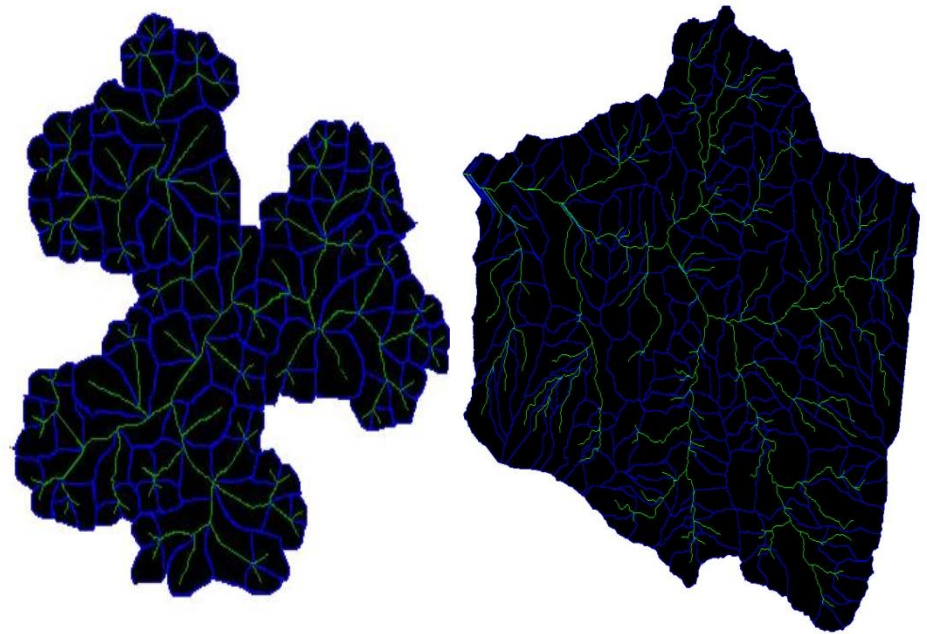
where A is the area of basin with main channel length L_{mc} .

- Hurst's law: $L_{\perp} \propto L_{\parallel}^H$
where L_{\parallel} is the longitudinal length and L_{\perp} transverse length respectively.

Allometric power-laws

- ∞ Allometric power-laws are derived between the basic measures such as basin area, basin perimeter, channel length, longitudinal length and transverse length
- ∞ Observed that these power-laws are of universal type as they exhibit similar scaling relationships at all scales.

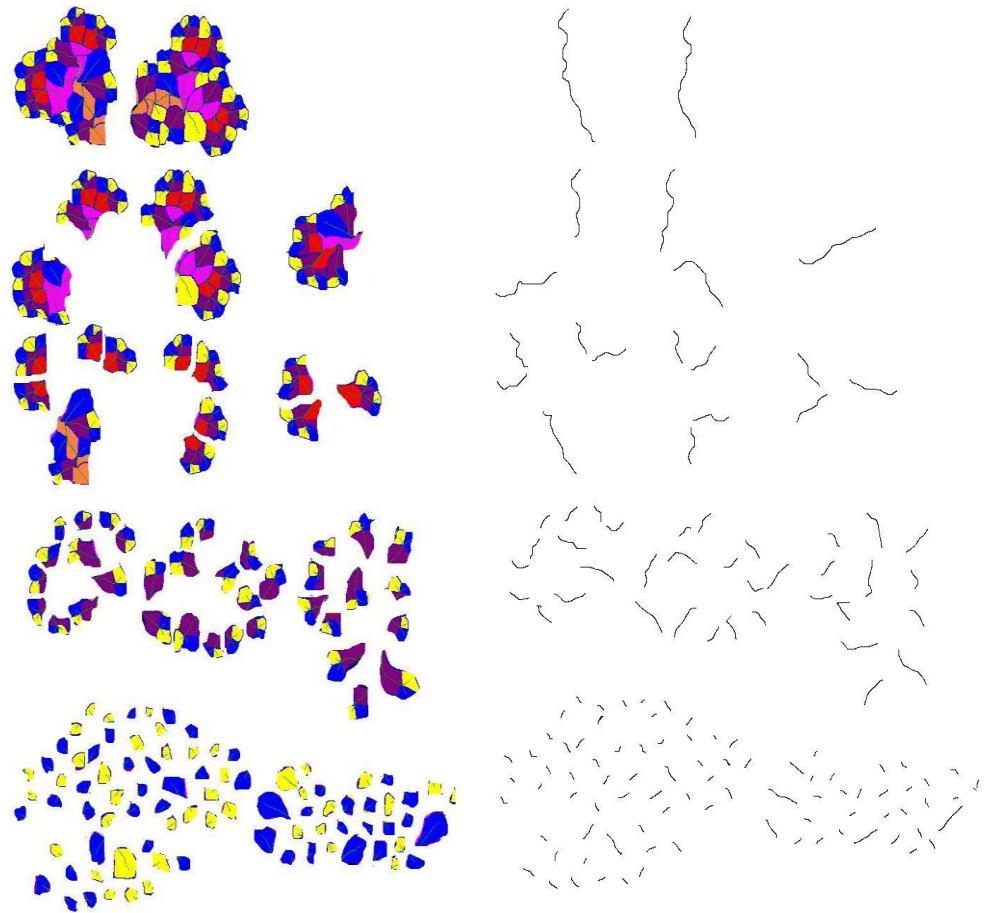
Existing allometric power-laws: Decomposed basins & networks



Existing allometric power-laws : Decomposed basins and networks

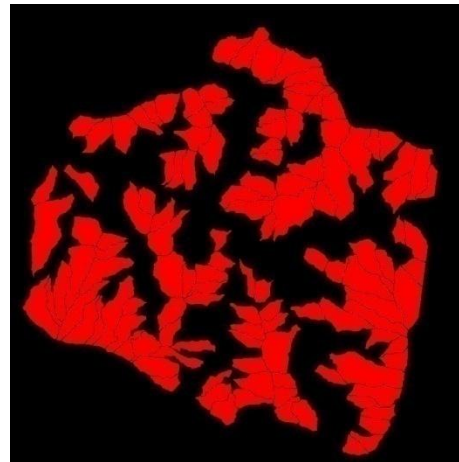
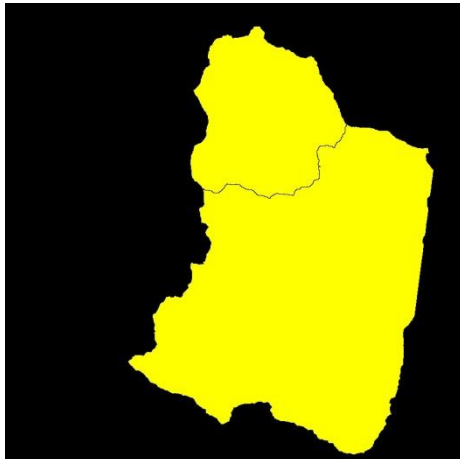
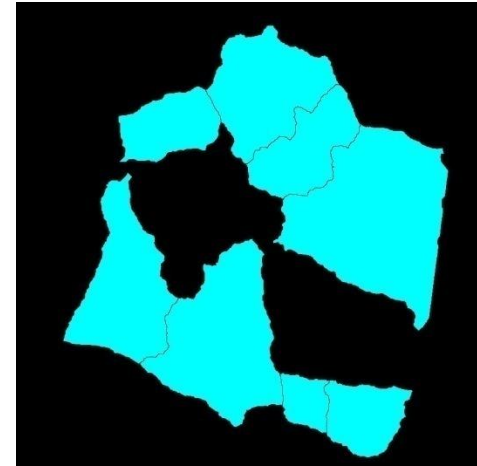
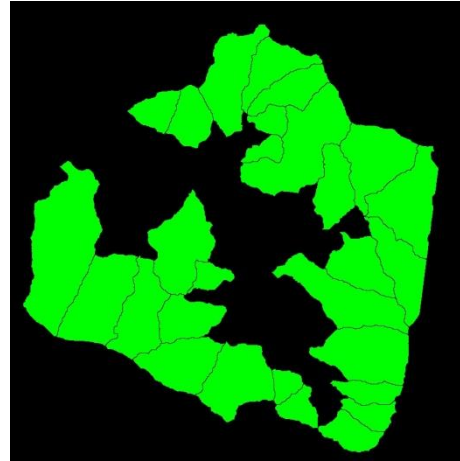
The number of decomposed sub-basins of respective orders from the simulated 6th order F-DEM include:

- two 5th
- five 4th
- ten 3rd
- thirty six 2nd, and
- eighty six 1st order basins.



Existing allometric power-laws :

Decomposed basins and networks



Decomposed sub-basins
are

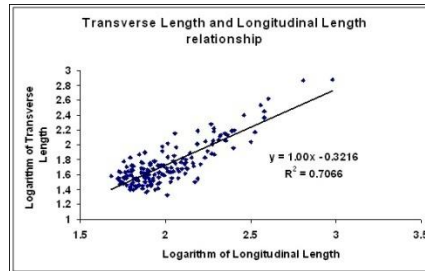
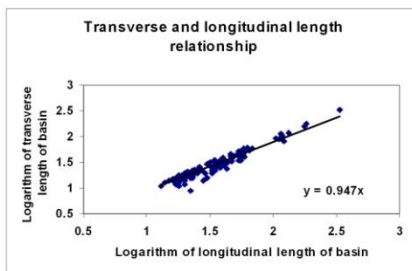
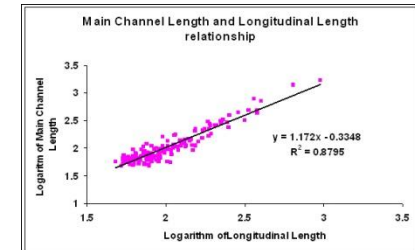
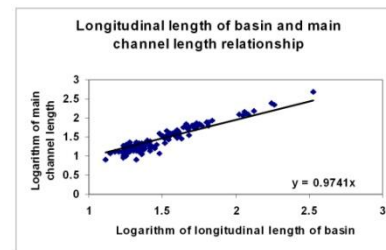
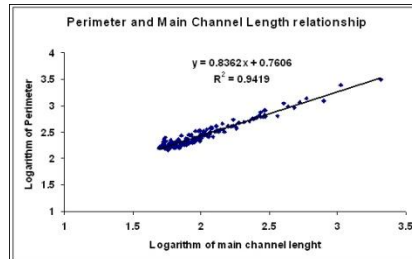
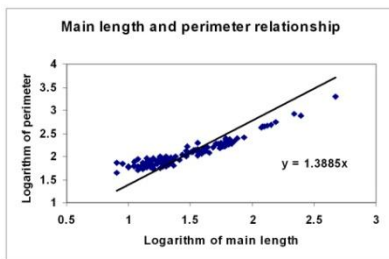
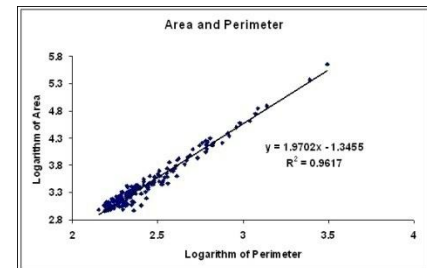
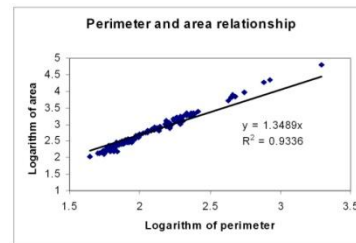
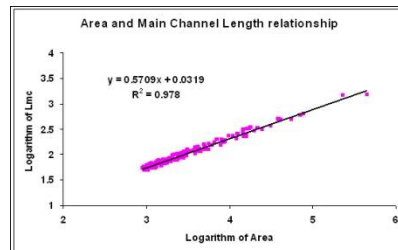
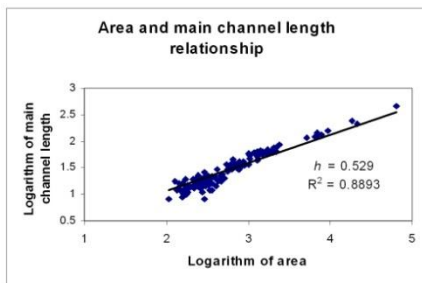
- two 4th
- eight 3rd
- twenty-eight 2nd, and
- one hundred twenty-four 1st
order basins.

Existing allometric power-laws : Basic Measures



Basic measures for a basin, (a) basin area, (b) total channel length, (c) main channel length, (d) basin perimeter, (e) longitudinal length and (f) transverse length.

Scale Invariant allometric power-laws



Allometric relationships among various areal and length parameters for all sub-basins of F-DEM and TOPSAR DEM.

Scale Invariant allometric power-laws

F-DEM

TOPSAR DEMs

Relations	Notations	For all orders	Basin's order					
			1	2	3	4	5	6
A and L_{mc}	h	0.53	0.502	0.56	0.56	0.55	0.55	0.56
A and P	α	1.35	1.31	1.36	1.41	1.44	1.48	1.46
P and L_{mc}	β	1.39	1.51	1.32	1.28	1.26	1.23	1.23
L_{mc} and $L_{ }$	-	0.97	0.92	1.01	1.04	1.03	0.94	0.95
L_{\perp} and $L_{ }$	H	0.95	0.94	0.94	0.96	0.98	0.94	0.98
2h	$D_{L_{mc}}$	1.06	1.00	1.11	1.11	1.10	1.10	1.12
$2/\alpha$	D_p	1.48	1.53	1.47	1.42	1.39	1.35	1.37
$1 + \frac{D_{L_{mc}}}{1+H}$	-	1.55	1.52	1.57	1.59	1.56	1.57	1.57

Relations	Notations	For all orders	Basin's order				
			1	2	3	4	5
A and L_{mc}	h	0.57	0.60	0.57	0.50	0.58	0.56
A and P	α	1.97	1.62	1.78	1.78	1.69	1.62
P and L_{mc}	β	0.84	0.78	0.92	0.88	1.09	1.05
L_{mc} and $L_{ }$	-	1.17	0.75	1.00	0.92	1.02	1.08
L_{\perp} and $L_{ }$	H	1.00	0.39	0.53	0.68	1.00	0.97
2h	$D_{L_{mc}}$	1.14	1.20	1.14	1.00	1.16	1.12
$2/\alpha$	D_p	1.02	1.23	1.12	1.12	1.18	1.23
$1 + \frac{D_{L_{mc}}}{1+H}$	-	1.57	1.86	1.74	1.60	1.58	1.57

Existing allometric power-laws : Scaling laws

Our results shown for basins derived from F-DEM and TOPSAR DEM are in good accord with power-laws derived from Optimal Channel Networks (Maritan et. al., 2002) and Random Self-Similar Networks (Veitzer and Gupta 2000) and certain natural river basins.

Novel scaling relationships between travel-time channel networks, convex hulls and convexity measures

Network topology and watershed geometry are important features in terrain characterization.

Travel-time networks are sequence of networks generated by removing the extremities of the network iteratively. Hit-or-Miss transformation and Thinning transformations is used in generating travel-time network. Half-plane closing-based algorithm (Soille, 2005) is employed to generate convex hulls for these travel-time networks.

Length of the travel-time network and area of the corresponding convex hull are used to derive new scaling exponents.

Proposed scaling relationships : Travel-time networks

- The process of deleting the end points from the networks is named as pruning.
- To decompose the stream network subsets from $n = 1$ to N , structuring template of B_1 and B_2 are decomposed into various subsets, B_n^i where $i = 1, 2, \dots, 8$ and $n = 1, 2$
- Both structuring templates are disjointed into eight directions. The intersecting portion of eroded S and eroded S_c by disjointed templates $\{B_1^k\}$ and $\{B_2^k\}$ $k = 1, 2, \dots, 8$ respectively are computed to derive pruned version of S .
- The X's in the structuring templates signifies the 'don't care' condition – it doesn't matter whether the pixel in that location has a value of 0 or 1.

	1 0 0	0 0 1	0 0 0	0 0 0
$B_1^1 =$	0 1 0	$B_1^2 =$ 0 1 0	$B_1^3 =$ 0 1 0	$B_1^4 =$ 0 1 0
	0 0 0	0 0 0	0 0 1	1 0 0
	X 1 X	0 0 X	0 0 0	X 0 0
$B_1^5 =$	0 1 0	$B_1^6 =$ 0 1 1	$B_1^7 =$ 0 1 0	$B_1^8 =$ 1 1 0
	0 0 0	0 0 X	X 1 X	X 0 0
	0 1 1	1 1 0	1 1 1	1 1 1
$B_2^1 =$	1 0 1	$B_2^2 =$ 1 0 1	$B_2^3 =$ 1 0 1	$B_2^4 =$ 1 0 1
	1 1 1	1 1 1	1 1 0	0 1 1
	X 0 X	1 1 X	1 1 1	X 1 1
$B_2^5 =$	1 0 1	$B_2^6 =$ 1 0 0	$B_2^7 =$ 1 0 1	$B_2^8 =$ 0 0 1
	1 1 1	1 1 X	X 0 X	X 1 1

Proposed scaling relationships : Travel-time networks

- ∞ Mathematically,

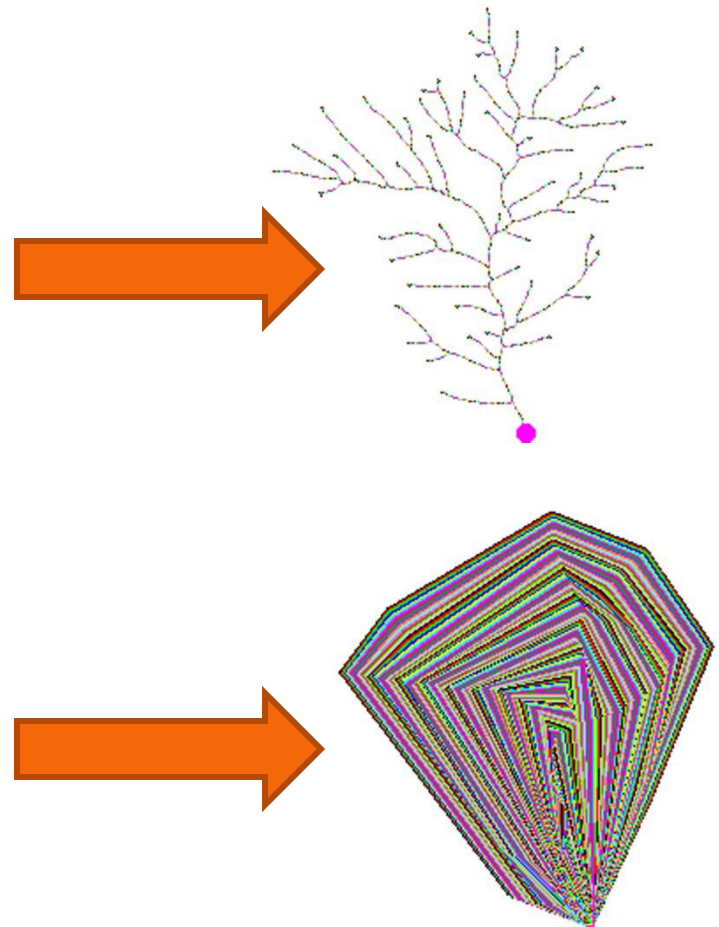
$$S * B = (S \ominus B_1^k) \cap (S^c \ominus B_2^k) \quad \text{where} \quad B = B_1^k \cup B_2^k$$
- ∞ By subtracting $(S * B)$ from S , a pruned version of S is obtained and expressed as
- ∞ $S_1 = S \otimes \{B\}$ where, $S \otimes \{B\} = S - (S * B)$
- ∞ $\{B\}$ is the sequence of $\{(B_1^1, B_1^2, \dots, B_1^8), (B_2^1, B_2^2, \dots, B_2^8)\}$
- ∞ After pruning of S in first pass with B_1 , the process continue with pruning with B_2 and so on until S is pruned in the last pass with B_8 .

$$S \otimes \{B\} = ((\dots((S \otimes B^1) \otimes B^2) \dots) \otimes B^8)$$
- ∞ The whole process removes the first-encountered open pixels of S and produces S_1 .
- ∞ Repeating the same process on S_1 will produce S_2 . The process is repeated until no further changes occur, where the closed outlet is reached.

Proposed scaling relationships : Convex hull

Convex hull is the smallest convex set that contains all the points of the network.

Since convex hull represents the basin of network, convex hulls of the travel-time networks are generated.



Proposed scaling relationships : Pruned network and convex hull

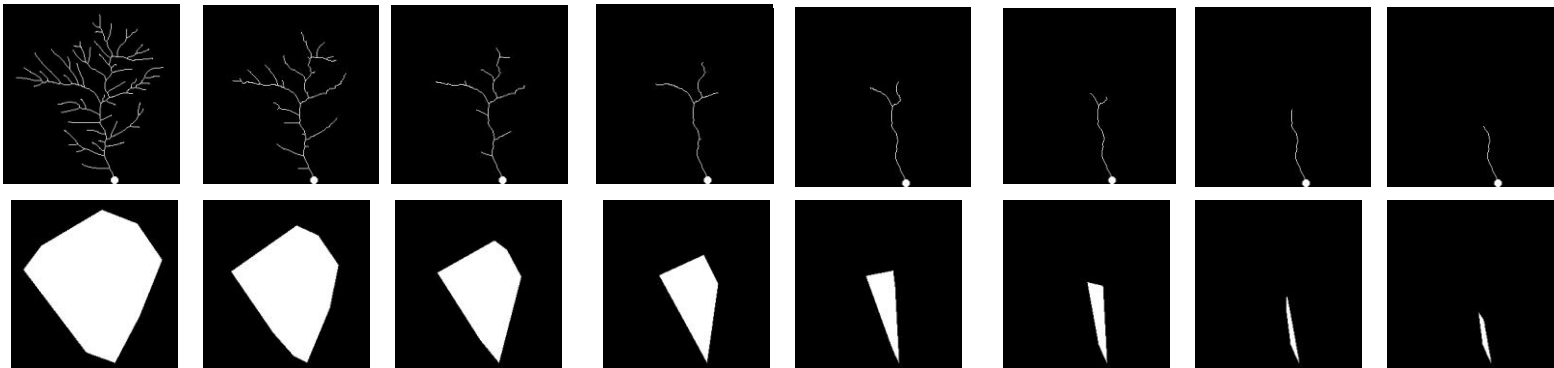
Properties of the pruned network:

$$1. S = \bigcup_{n=0}^{N-1} (S_n - S_{n+1})$$

$$2. S_N \subset S_{N-1} \subset \dots \subset S_2 \subset S_1 \subset S$$

3. S, S_1, S_2, \dots, S_N obtained by iterative **pruning**.

The final convex polygon containing all the points of S yields $C(S)$.



Proposed scaling relationships

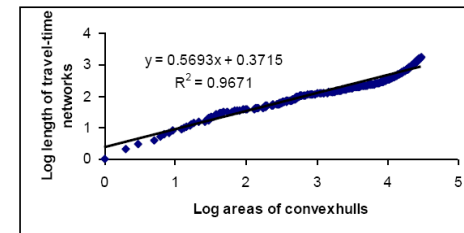
- Network – pruning – network length = S_n
- Convex hull computed – convex hull area = $C(S_n)$
- Convexity measures, $CM =$ ratio between the areas of S_n and $C(S_n)$.

$$L(S_n) \sim A[C(S_n)]^\alpha$$

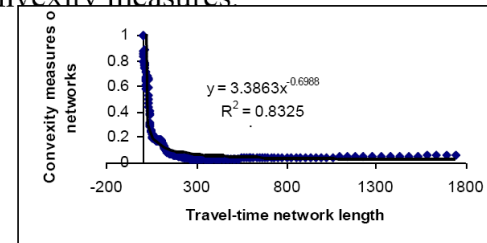
$$CM(S_n) \sim \frac{1}{L(S_n)^\beta}$$

$$CM(S_n) \sim \frac{1}{A[C(S_n)]^\lambda}$$

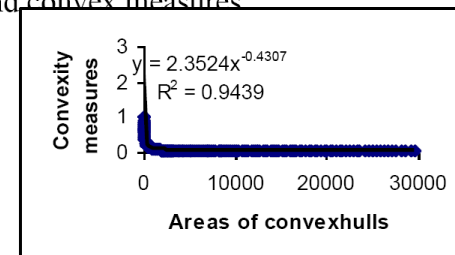
Graph of lengths of the sequential pruned networks versus the corresponding areas of convex hulls.



Relationship between channel lengths and convexity measures.

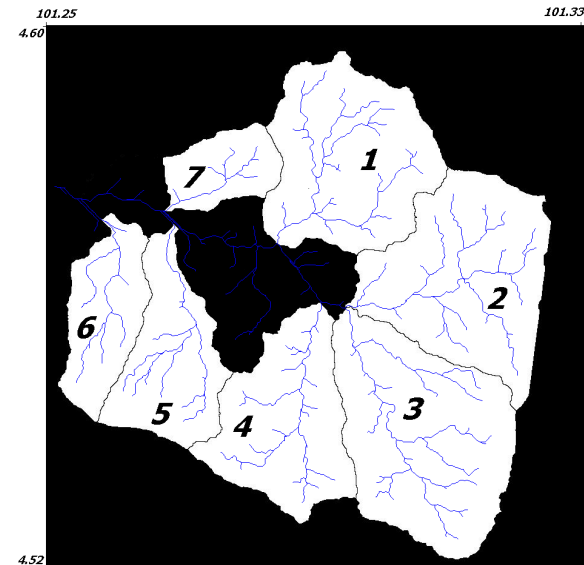
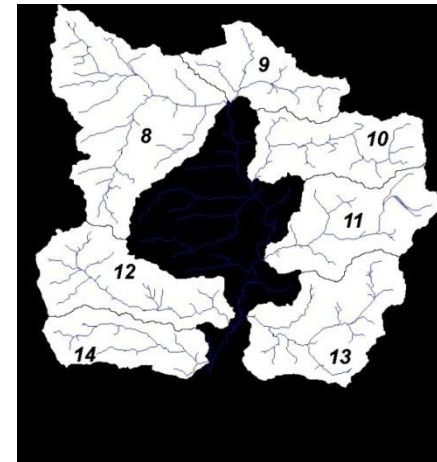
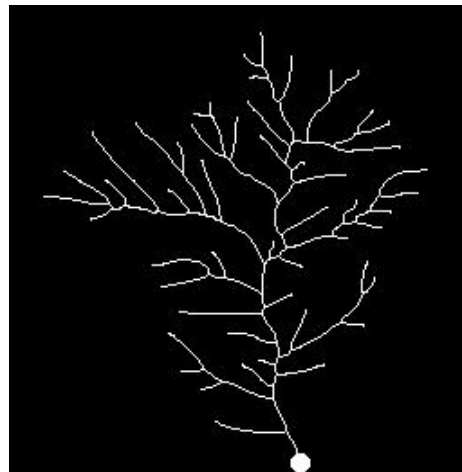
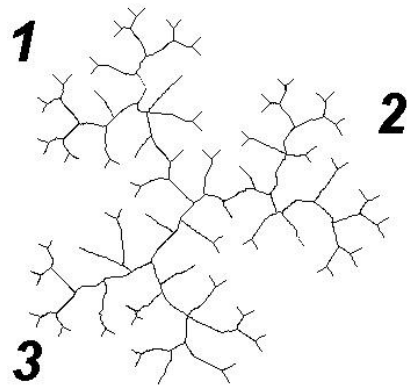


Relationship between areas of convex hulls and convex measures.



Proposed scaling relationships

- Sample basin
- Simulated F-DEM basins
- Cameron basins
- Petaling basins



Proposed scaling relationships

Network	$\alpha, (R^2)$	σ, R^2	λ, R^2	R_b	R_l	h	H
Sample	0.5693, (0.9671)	0.6988, (0.8325)	0.4307, (0.9439)	3.84	1.66	-	-
Basin 1 (Cameron)	0.5777, (0.9883)	0.7109, (0.9358)	0.4223, (0.9783)	3.60	2.21	0.5414	0.9714
Basin 2 (Cameron)	0.5774, (0.9925)	0.7189, (0.9586)	0.4226, (0.9861)	4.35	2.25	0.5561	1
Basin 3 (Cameron)	0.5799, (0.9934)	0.7131, (0.963)	0.4201, (0.9875)	3.31	2.39	0.5612	0.9256
Basin 4 (Cameron)	0.5521, (0.9835)	0.7814, (0.92)	0.4479, (0.9752)	4.47	3.18	0.5671	0.9506
Basin 5 (Cameron)	0.5798, (0.9905)	0.7083, (0.9469)	0.4202, (0.982)	3.31	2.16	0.5766	0.9162
Basin 6 (Cameron)	0.5819, (0.9865)	0.6955, (0.925)	0.4181, (0.9743)	4.00	2.64	0.5746	0.8597
Basin 7 (Cameron)	0.5885, (0.9887)	0.68, (0.9348)	0.4115, (0.9772)	2.82	2.39	0.5548	0.895
Basin 1 (Petaling)	0.5462, (0.969)	0.7741, (0.8561)	0.4538, (0.9557)	5.00	2.57	0.5568	0.9319
Basin 2 (Petaling)	0.5393, (0.9899)	0.8357, (0.9532)	0.4607, (0.9863)	4.00	3.51	0.5828	0.8623
Basin 3 (Petaling)	0.5198, (0.9852)	0.8953, (0.9367)	0.4802, (0.9827)	4.24	3.30	0.597	0.9019
Basin 4 (Petaling)	0.5592, (0.9938)	0.7771, (0.9684)	0.4408, (0.99)	4.24	2.96	0.5807	0.8902
Basin 5 (Petaling)	0.5729, (0.9906)	0.729, (0.9492)	0.4271, (0.9832)	4.79	3.96	0.5844	0.8704
Basin 6 (Petaling)	0.5547, (0.9872)	0.7798, (0.937)	0.4453, (0.9804)	4.89	3.42	0.5713	0.9116
Basin 7 (Petaling)	0.6059, (0.9929)	0.6387, (0.9551)	0.3941, (0.9834)	3.60	3.39	0.5865	0.8312

Allometric power-laws between travel-time channel networks, convex hulls, and convexity measures for model network, networks of Hortonian fractal DEM, and networks of fourteen basins of Cameron Highlands and Petaling region.

Proposed scaling relationships

These proposed scaling exponents are shown for basins derived from simulated F-DEM and TOPSAR DEMs.

These exponents are scale-independent.

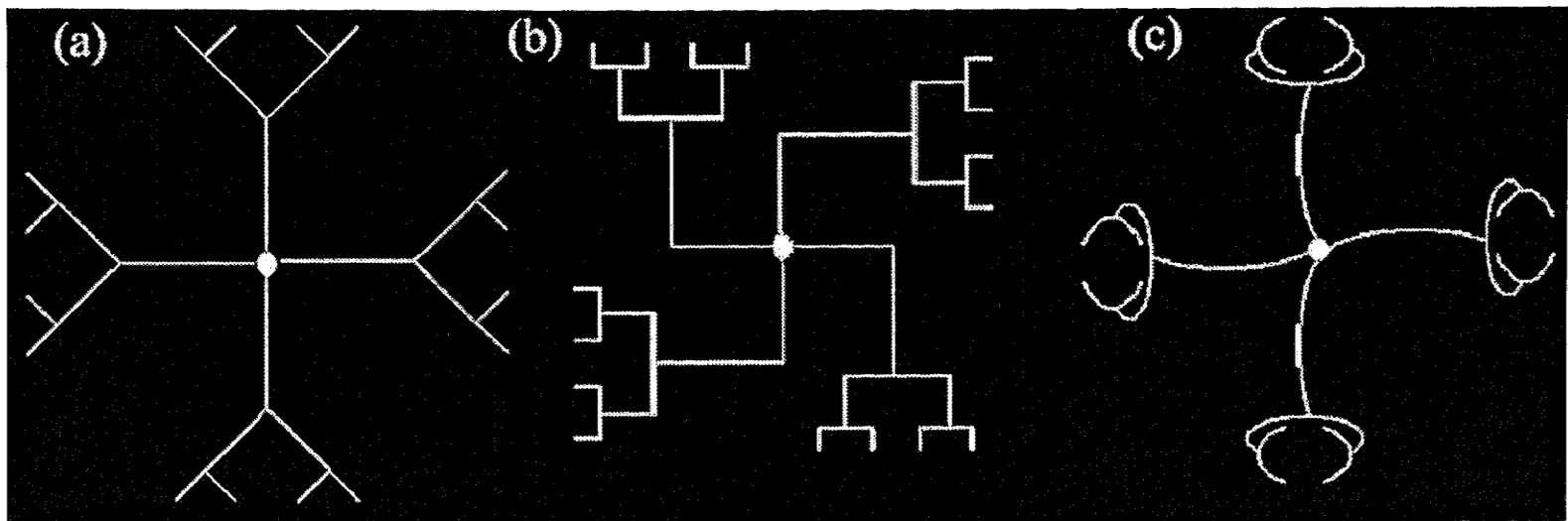
At macroscopic level, these exponents complement with other existing scaling coefficients can be used to identify commonly sharing generic mechanisms in different river basins.

II.II.II. Scale Invariant But Shape Dependent Power-laws

Objectives

To propose morphology based method via fragmentation rules to compute scale invariant but shape-dependent measures of non-network space of a basin.

To make comparisons between morphometry based parameters / dimensions and dimensions derived for non-network space.



Topologically Invariant networks with variant geometric organization

Proposed Technique

Step1: Channel network is traced from topographic map.

Step2: Channel network is dilated and eroded iteratively until the entire basin is filled up with white space. This step is to generate catchment boundary automatically. Dilation followed by erosion is called structural closing, which will smoothen the image.

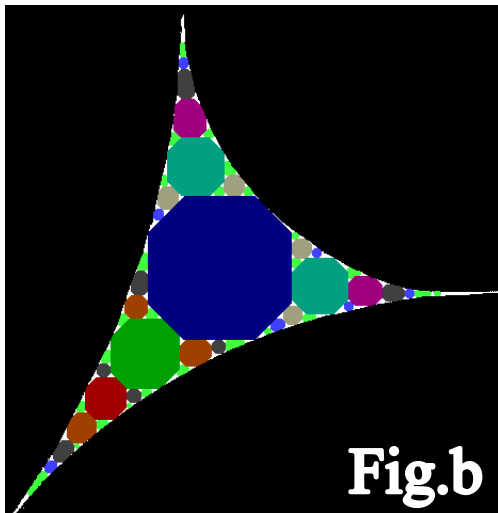
Step3: Generate the basin with channel network and non-network space with boundary by subtracting the channel network from the catchment boundary achieved in Step2.

Step4: Structural opening (erosion followed by dilation) is performed recursively in basin achieved in Step3 to fill the entire basin of non-network space with varying size of octagons.

Step5: Assign unique color for each size of octagons.

Step6: Compute morphometry for the basin.

Step7: Compute shape dependent dimension.



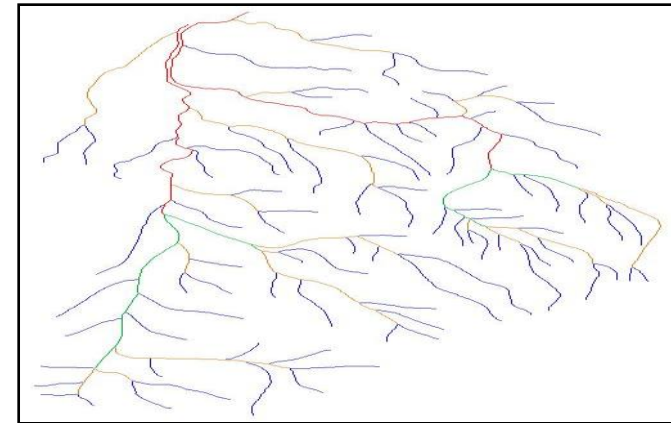
Power law relationship

- As per the previous fig. the slopes of the best-fit lines (α_N and α_A) for number-radius and area-radius relationships yield 2.37 and 1.34.
- These slope values of the best-fit lines provide shape dependent dimensions as $D_N = \alpha_N - 1$ and $D_A = \alpha_A$.
- As in previous Fig., D_N and D_A for non-network space yield 1.37 and 1.34.
- A Power-law relationship is shown in earlier Fig. with an exponent value 1.79 between the area and number of NODs observed with increasing radius of structuring template.

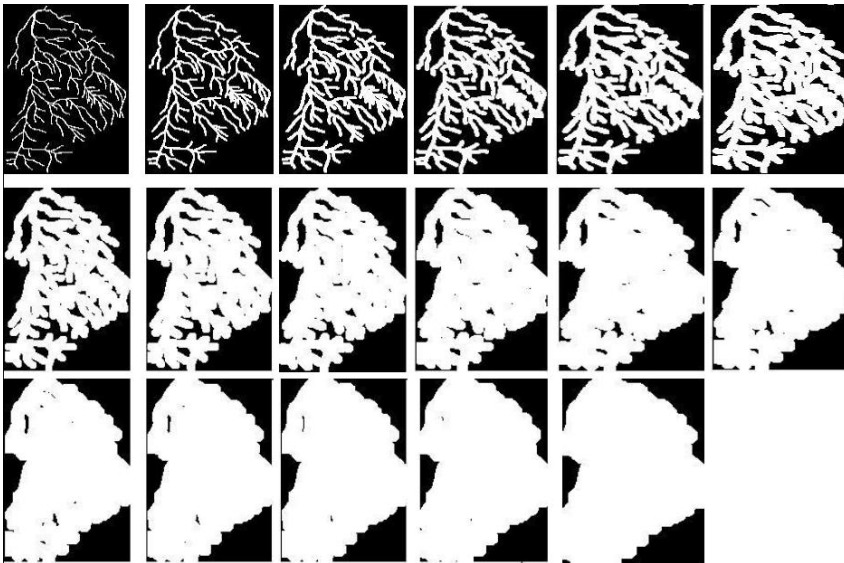
(a) Appollonian Space, and (b) after decomposition by means of octagon.

Algorithm Implementation:

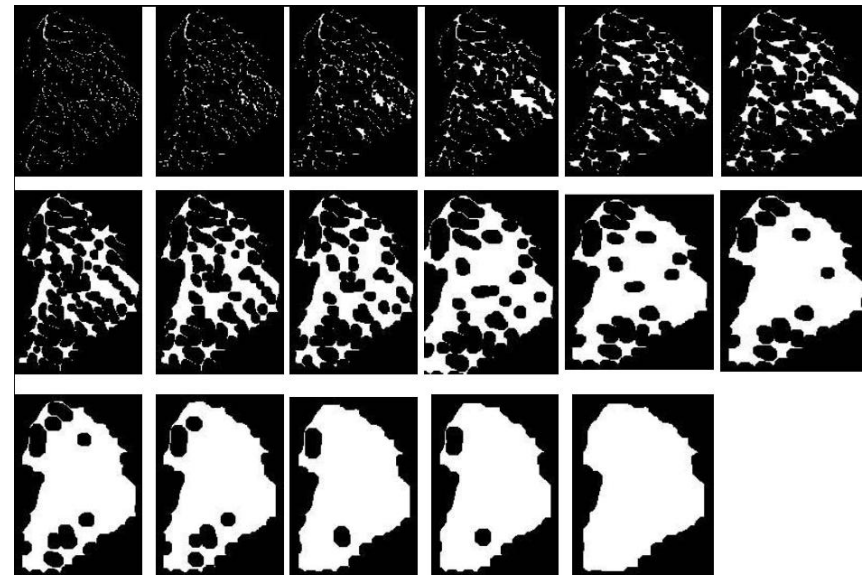
Step 1: **Channel network of sub basin 1**



Step 2: **Close-Hull Generation**



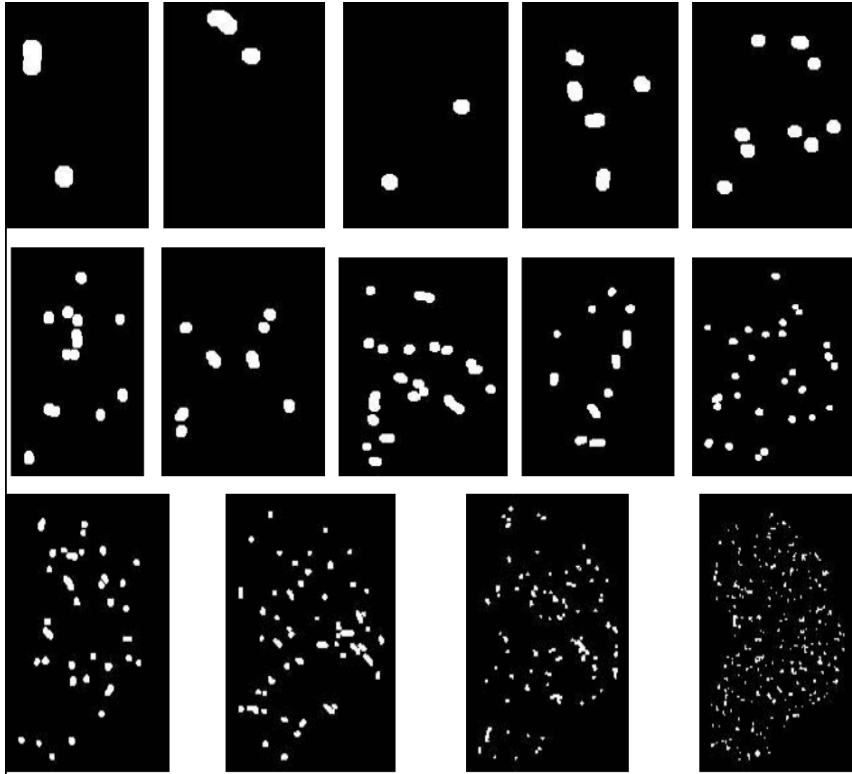
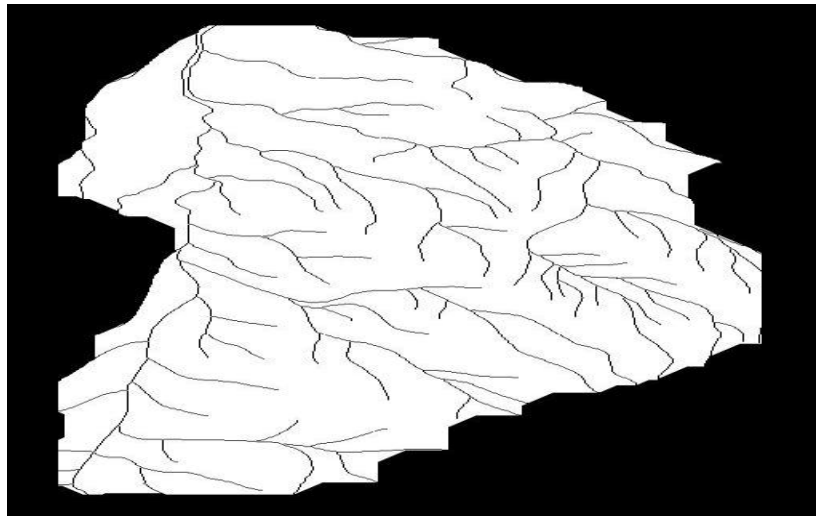
Iterative dilation of channel network of basin 1



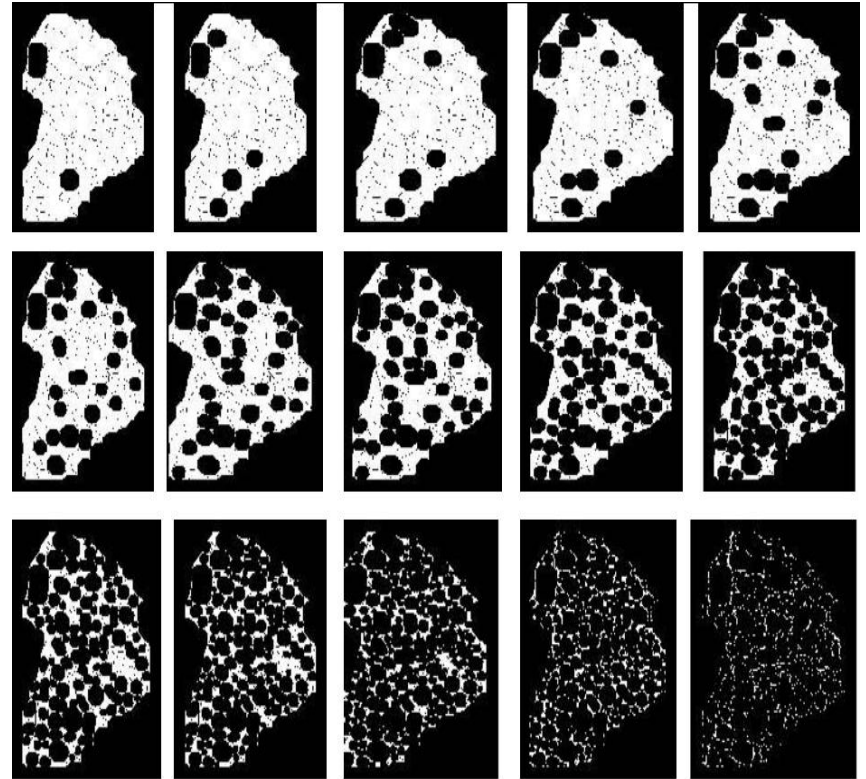
Iterative erosion applied to previous Fig

Step 3: Non-network space of basin 1

Iterative erosion applied to step-3 Fig.

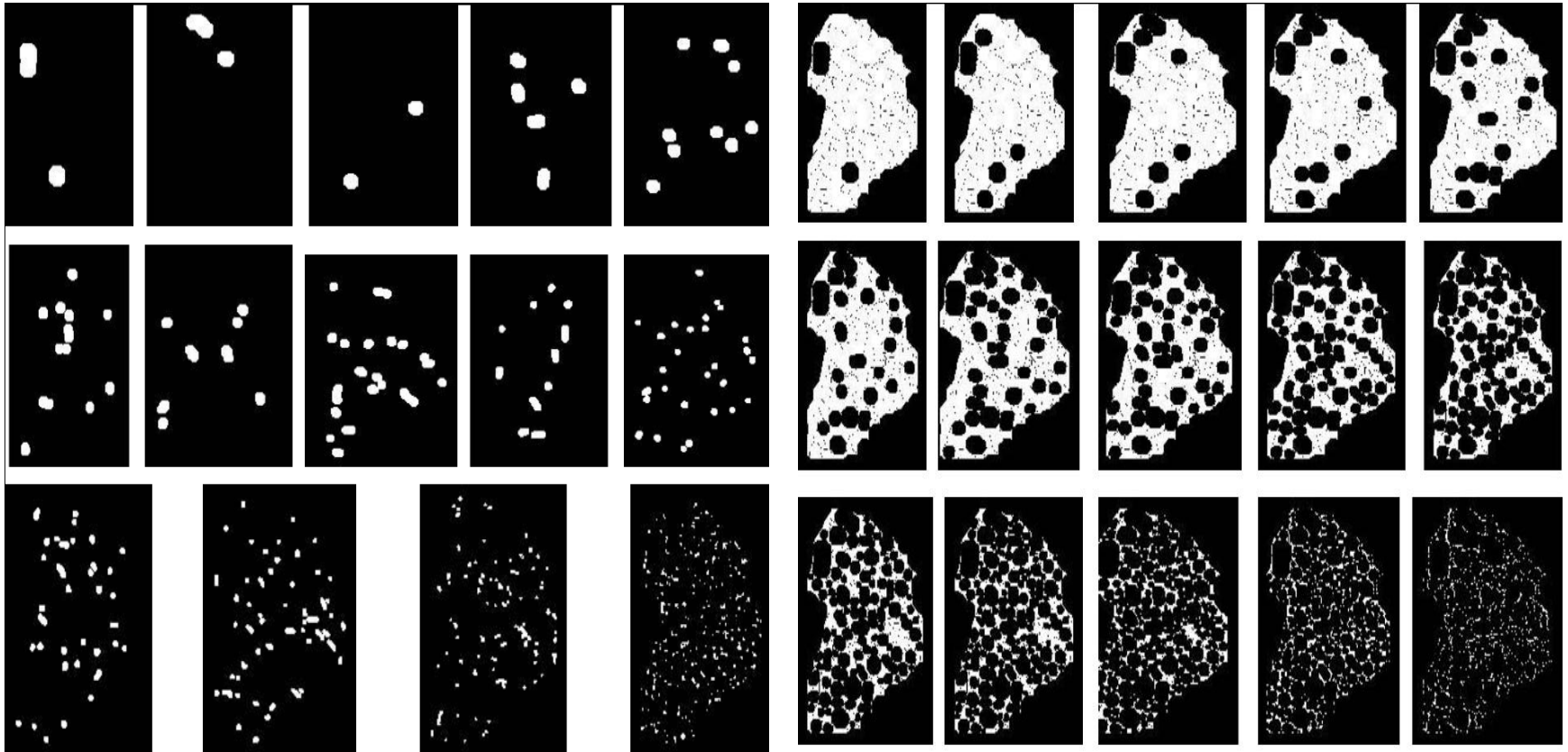


Iterative erosion applied to previous Fig.



Iterative dilation applied to previous Fig.

Step 4: Non-Network Space Decomposition

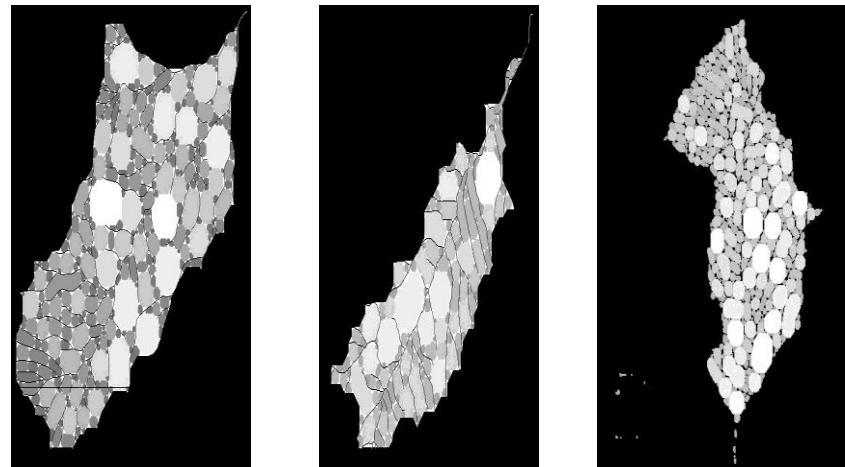
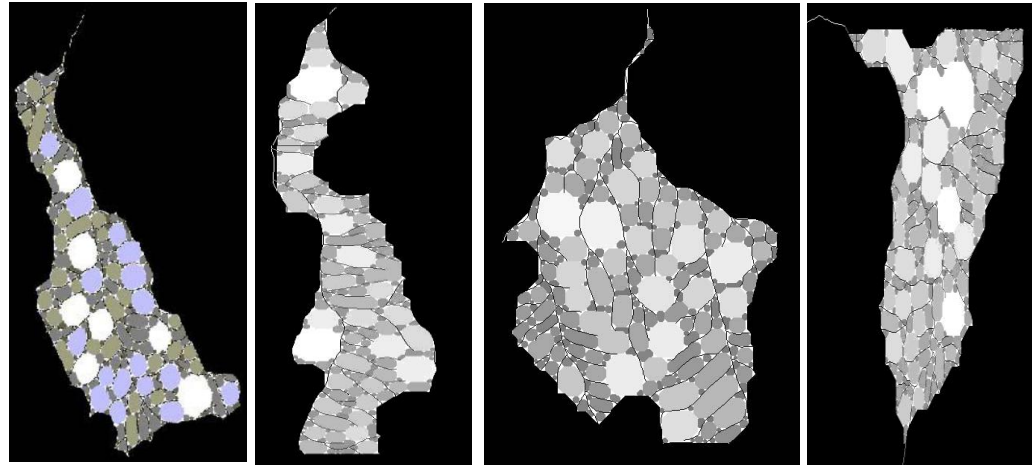
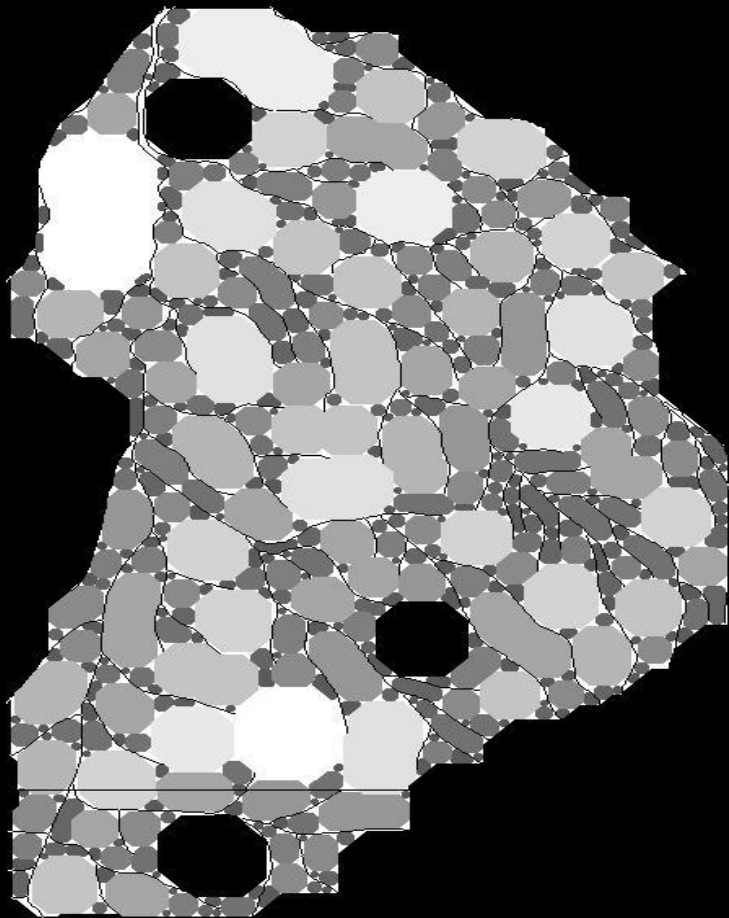


Iterative erosion applied to previous Fig.

Iterative dilation applied to previous Fig.

Decomposition of Non-network space in to non-overlapping disks of octagon shape of several sizes for basin 1

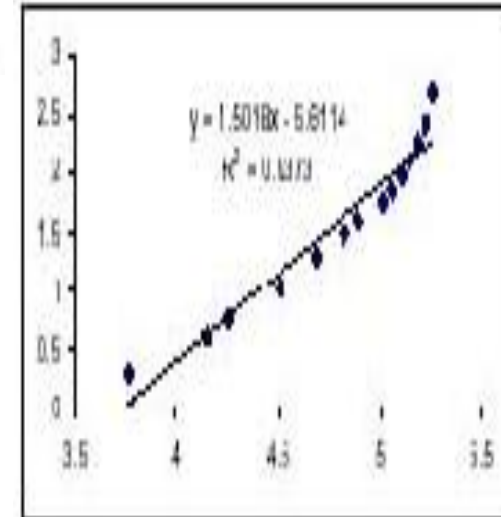
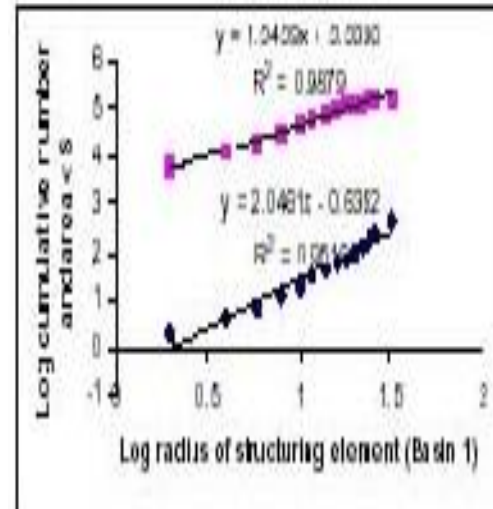
Non-Network Spaces Packed with Non-Overlapping Disks of basins 2 to 8



Dimensions derived from morphometry of network and non network space

Morphometric parameter computations achieved through decomposition of non-network space

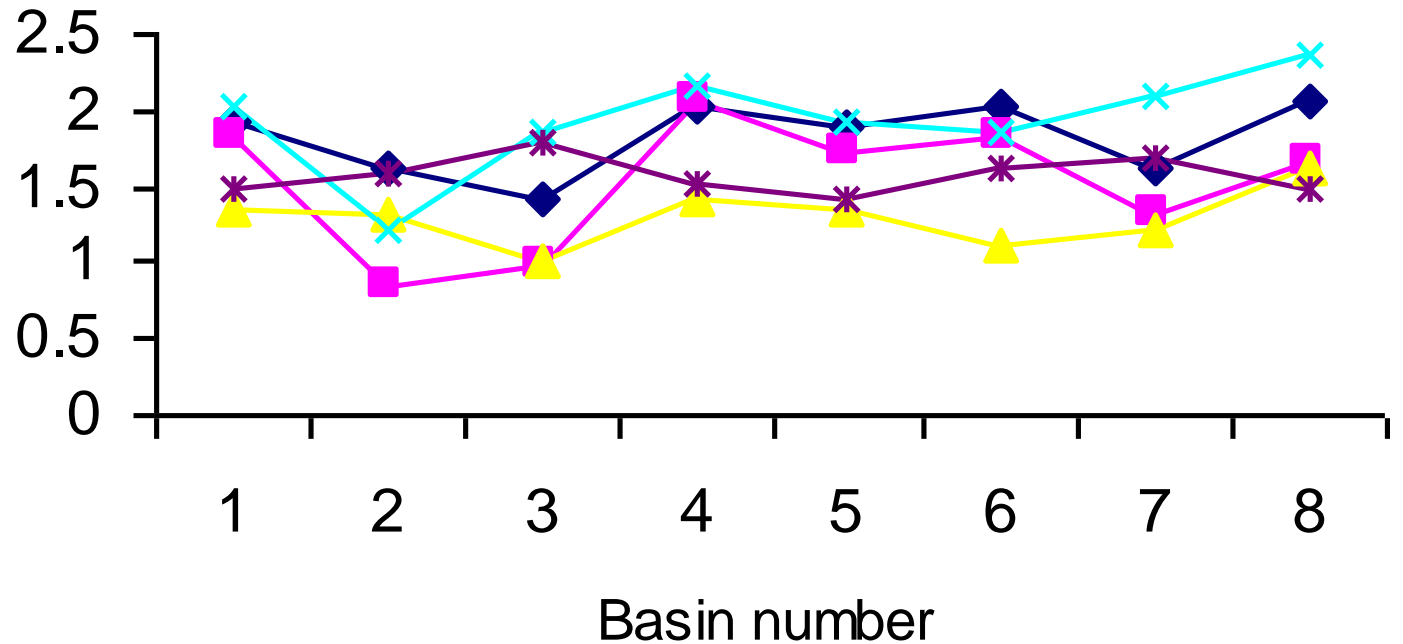
Basin #	Network FD	Log R _S /Log R _N	R vs A	R vs N	A vs N
1	1.83	1.93	1.34	2.06	1.50
2	0.86	1.63	1.33	1.23	1.59
3	0.98	1.41	1.02	1.87	1.80
4	2.07	2.01	1.43	2.17	1.52
5	1.73	1.90	1.34	1.94	1.43
6	1.84	2.04	1.13	1.87	1.63
7	1.33	1.61	1.23	2.08	1.70
8	1.65	2.06	1.61	2.38	1.49



Basin number versus varied dimensions derived from morphometry of networks and non-network spaces

Series1 Series2 Series3 Series4 Series5

Dimensions
computed through
morphometry of
network and non-
network space



II.II.III. Granulometric analysis of digital topography

Granulometric analysis

Morphological multiscaling transformations are shown to be a potential tool in deriving meaningful terrain roughness indexes.

Consider two different basins of two different physiographic setups (fluvial and tidal) that possess similar topological quantities, i.e., their networks may be topologically similar to each other. But the processes involved therein may be highly contrasting due to their different physiographic origins. Under such circumstances, the results that exhibit similarities in terms of topological quantities and scaling exponents would be insufficient to make an appropriate relationship with involved processes.

Therefore, granulometric approach is proposed to derive shape-size complexity measures of basins. This approach is based on probability distribution functions computed for both protrusions and intrusions (in other words *supremums* and *infimums*) of various degrees of sub-basins.

This granulometry-based technique is tested on sub-basins with various sizes and shapes decomposed from DEMs of two distinct geomorphic regions.

Granulometric Analysis

- Multi-scale opening till completely black
- Multi-scale closing till completely white
- Subtraction
- Probability function

$$PS_f(-n, B) = A[(f \bullet B_n) - (f \bullet B_{n-1})], 1 \leq n \leq K$$

$$PS_f(+n, B) = A[(f \circ B_n) - (f \circ B_{n+1})], 0 \leq n \leq N$$

- Average size

$$ps(n, f) = \frac{A(f \circ B_n) - A(f \circ B_{n+1})}{A(f \circ B_0)}, n = 0, 1, 2, \dots, N$$

$$ps(-n, f) = \frac{A(f \bullet B_n) - A(f \bullet B_{n-1})}{A(f \bullet B_K) - A(f \bullet B_0)}, n = 1, 2, \dots, K$$

- Average roughness

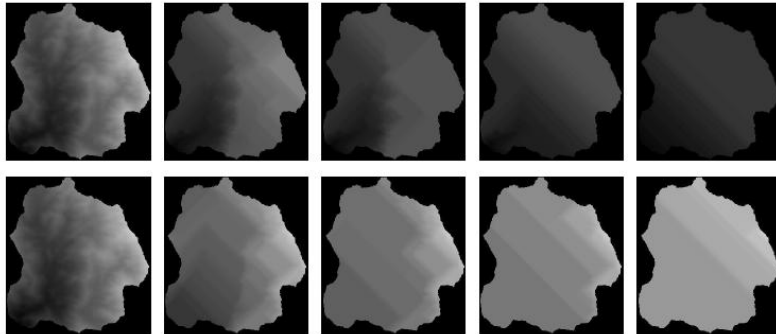
$$AS(f / B) = \sum_{n=0}^N nps(n, f)$$

$$H(f / B) = -\sum_{k=0}^n ps(n, f) \log ps(n, f)$$

Anti(Granulometric) Analysis

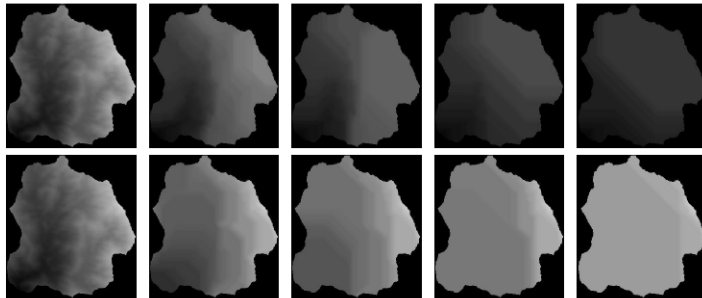
Multiscale opening/closing by rhombus

- Scale 1 , 40, 80, 120, 160



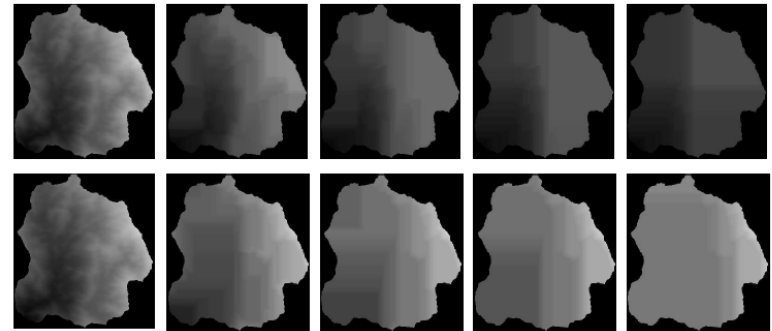
Multiscale opening/closing by octagon

- Scale 1 , 30, 60, 90, 120



Multiscale opening/closing by square

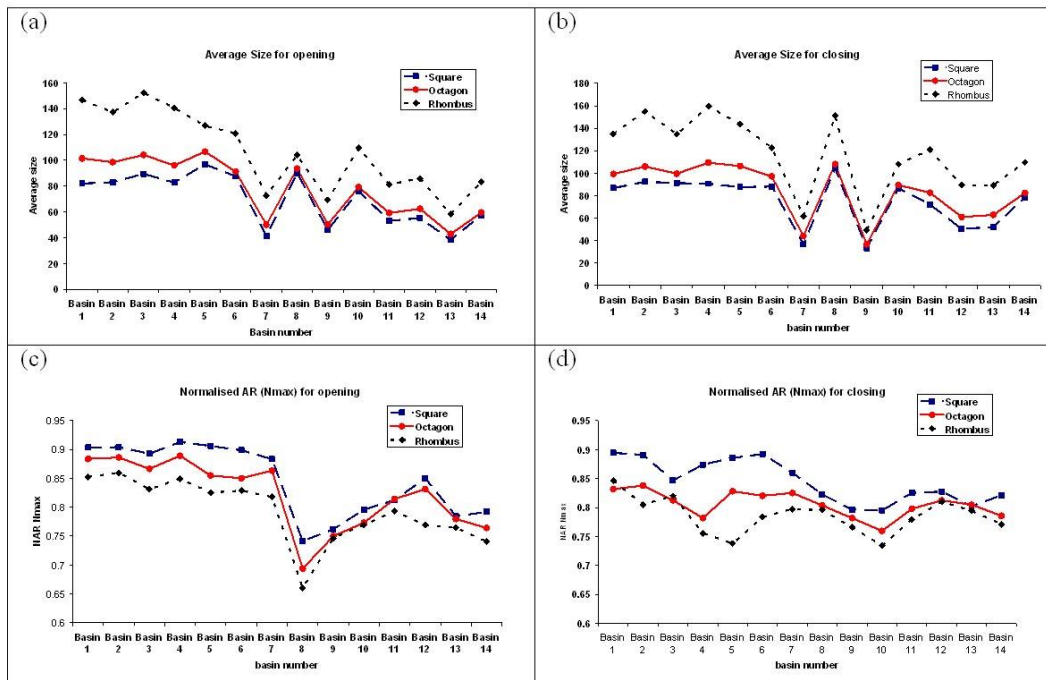
- Scale 1 , 20, 40, 60, 80



Granulometric analysis : Basin wise analysis

∞ Average size – 14 sub-basins

∞ Average roughness – 14 sub-basins



Granulometric Analysis : Basin wise analysis

The number of iterations required to make each sub-basin either become darker or brighter depends on the size, shape, origin, orientation of considered primitive template used to perform multiscale openings or closings, and also on the size of the basin and its physiographic composition. More opening/closing cycles are needed when structuring element rhombus is used, and it is followed by octagon and square.

Mean roughness indicates the shape-content of the basins. If the shape of SE is geometrically similar to basin regions, the average roughness result possesses lower analytical values. If the topography of basin is very different from the shape of SE, high roughness value is produced, which indicates that the basin is rough relative to that SE. In general, all basins are rougher relative to square shape as highest roughness indices are derived when square is used as SE.

A clear distinction is obvious between the Cameron and Petaling basins. Generally, roughness values of Cameron basins are significantly higher than that of Petaling basins.

The terrain complexity measures derived granulometrically are scale-independent, but strictly shape-dependent. The shape dependent complexity measures are sensitive to record the variations in basin shape, topology, and geometric organisation of hillslopes.

Granulometric analysis of basin-wise DEMs is a helpful tool for defining roughness parameters and other morphological/topological quantities.

III. Mathematical Morphology in GISci

Spatial Interpolations

Spatial Reasoning

- Strategic set identification
- Directional Spatial Relationship
- Point-to-Polygon Conversion

III.I. Spatial Interpolations

VISUALIZATION OF SPATIO-TEMPORAL BEHAVIOUR
OF DISCRETE MAPS VIA GENERATION OF
RECURSIVE MEDIAN ELEMENTS

Outline

Mathematical Morphological Transformations
employed include:

**Hausdorff Dilation, Hausdorff Erosion,
Morphological Median Element Computation, and
Morphological Interpolation.**

Objectives

To show relationships between the layers depicting noise-free phenomenon at two time periods.

To relate connected components of layers of two time periods via FOUR possible categories of spatial relationships of THREE groups.

To propose a framework to generate recursive interpolations via median set computations.

To demonstrate the validity of the framework on epidemic spread.

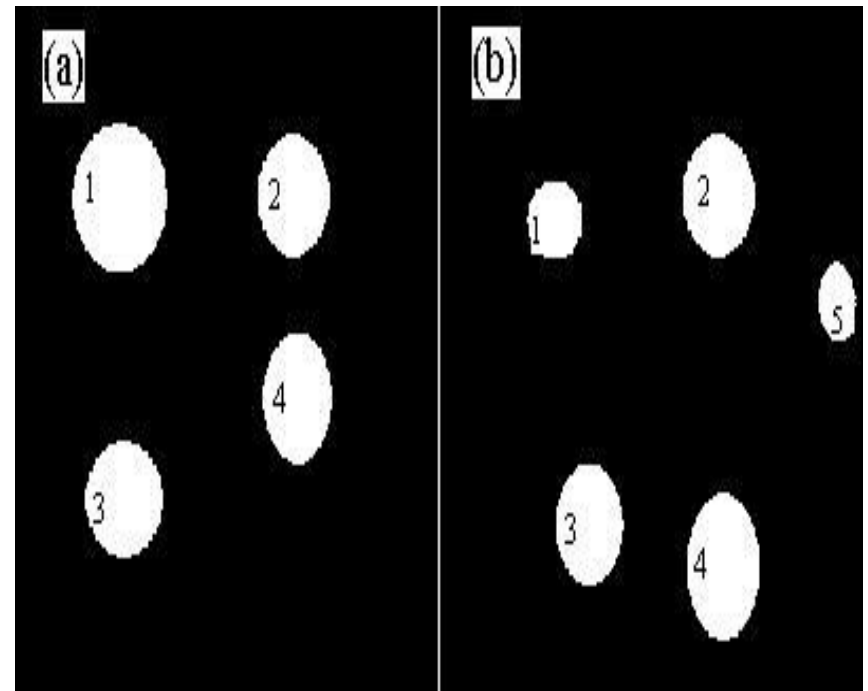
THREE Groups and FOUR Categories??

Three groups are conceived by checking the intersection properties between the corresponding connected components.

Four categories under the above three groups are visualized via logical relationships and Hausdorff erosion and Hausdorff dilation distances.

What are these Hausdorff distances?

What basics do we require to know to compute these distances?



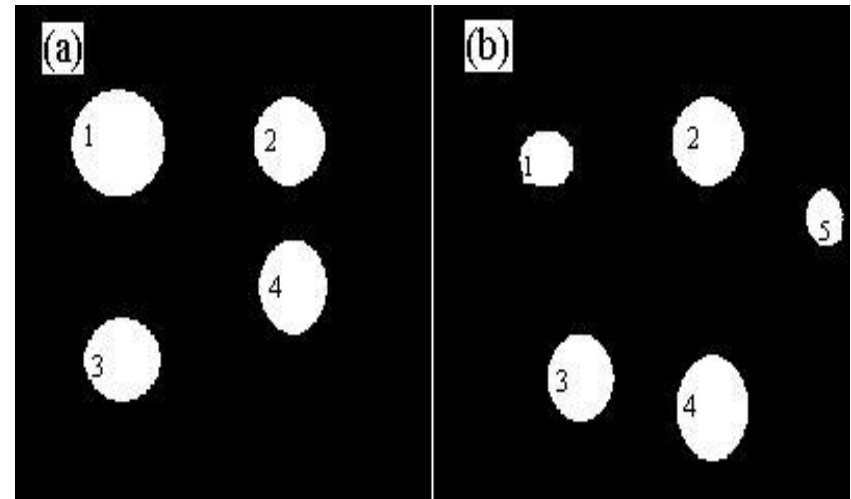
Spatial Relationships Between Sets and Their Categorization

∞ *Ordered sets.*

semi-ordered sets, if subsets of X^t (resp. X^{t+1}) are only partially contained in the other set X^{t+1} (resp. X^t).

Whereas, (X^t) and (X^{t+1}) are **considered** as **disordered sets** if there exists an empty set while taking the intersection of (X^t) and (X^{t+1}) (or) of their corresponding subsets.

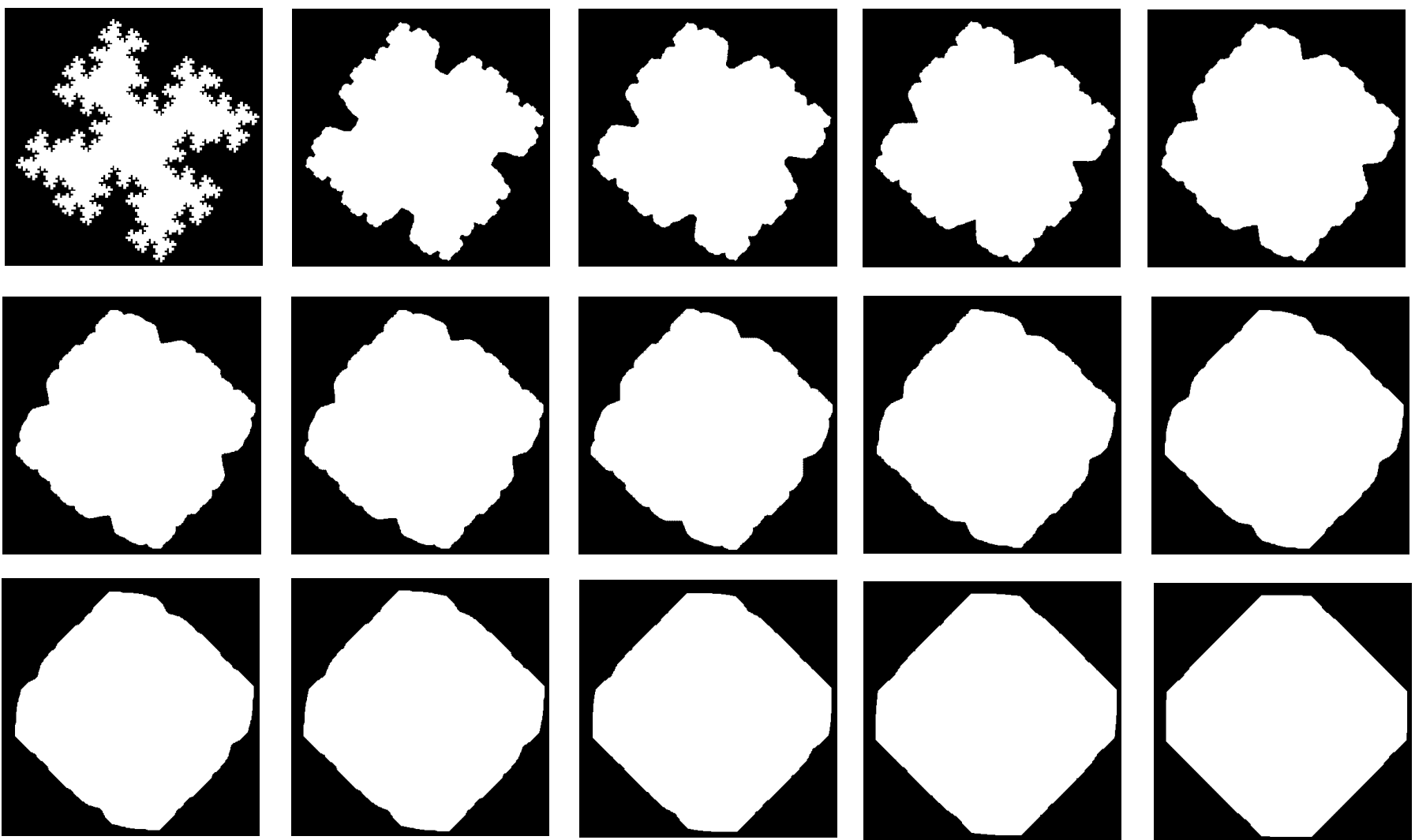
Description of categories via logical relations



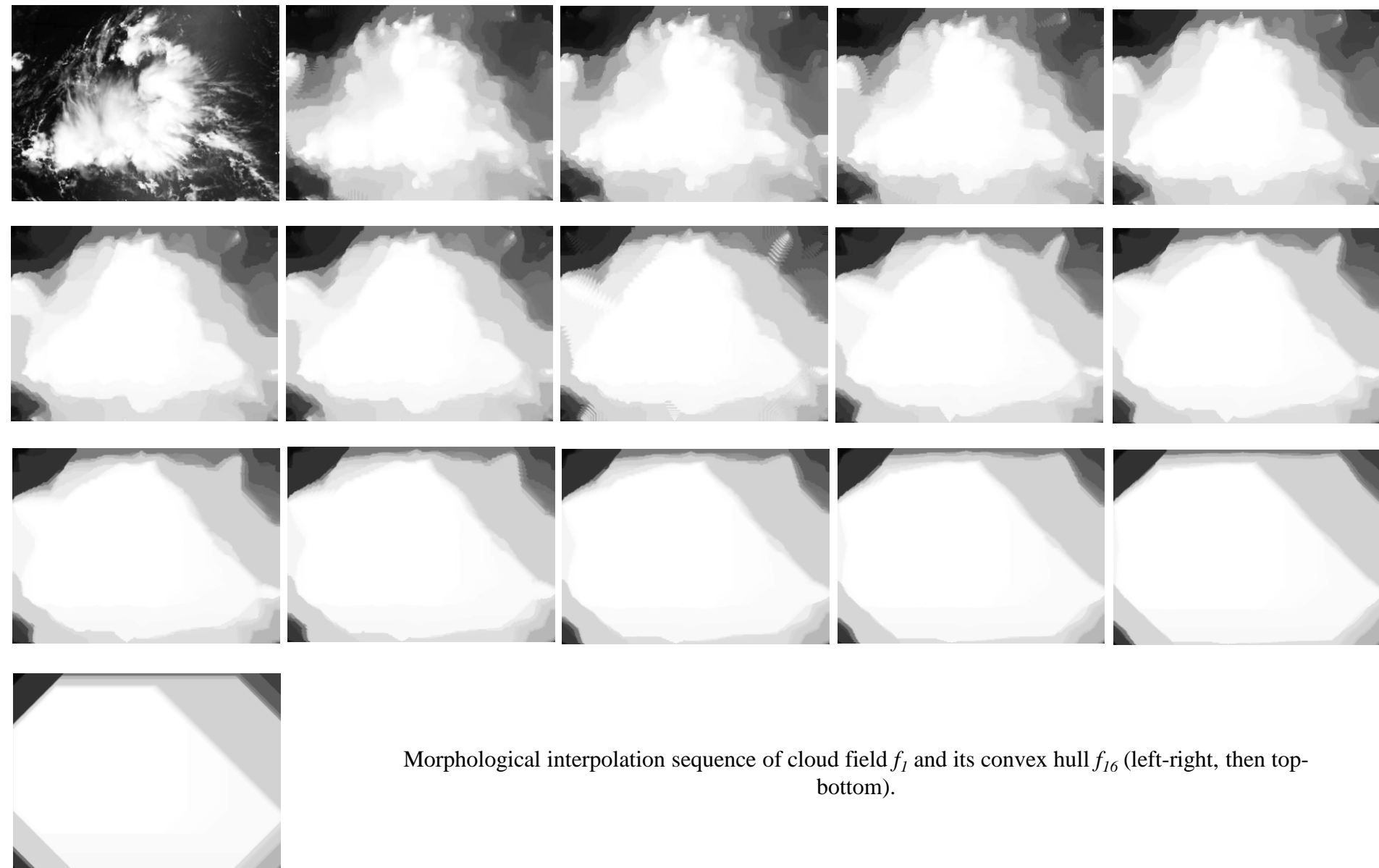
Categories via Hausdorff Erosion and Dilation Distances

TABLE 1. CATEGORY-WISE HAUSDORFF DISTANCES

Group	Category	$\sigma(X_i^t, X_i^{t+1})$	$\rho(X_i^t, X_i^{t+1})$
I	1	0	0
I	2	≥ 1	≥ 1
II	3	Does not exist	≥ 1
III	4	Does not exist	Does not exist



Morphological interpolation sequence of fractal M_1 and its convex hull M_{16} (left-right, then top-bottom).



Morphological interpolation sequence of cloud field f_l and its convex hull f_{l6} (left-right, then top-bottom).

Interpolated Sequence of Lakes' Data of Two Seasons

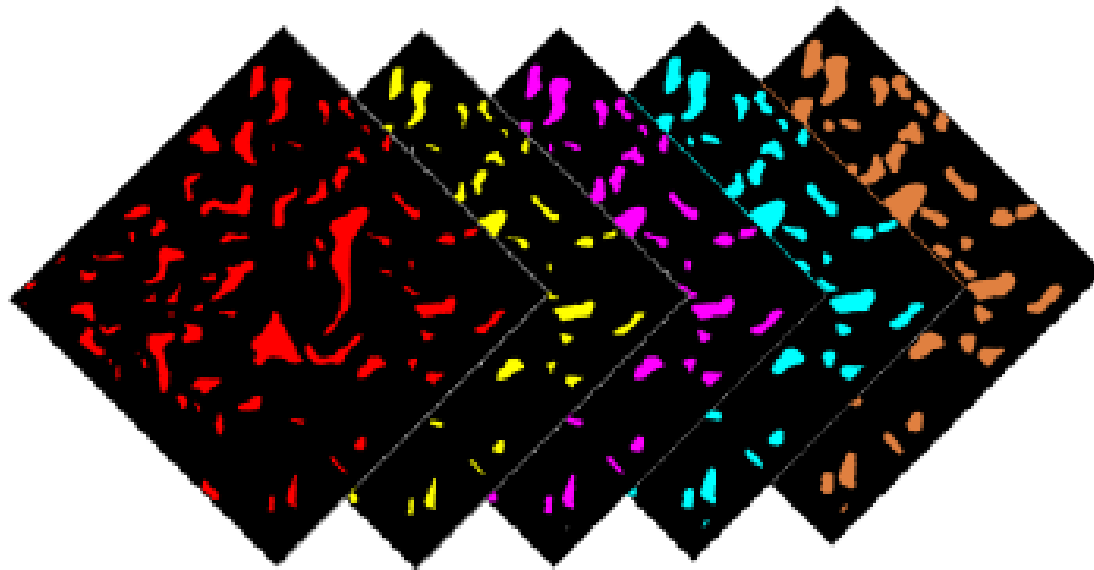
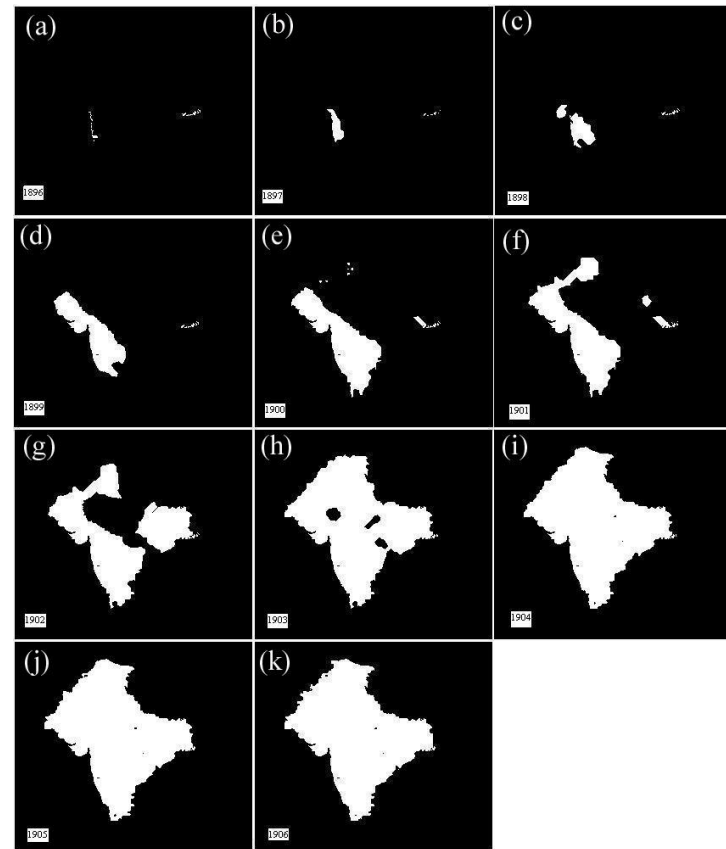
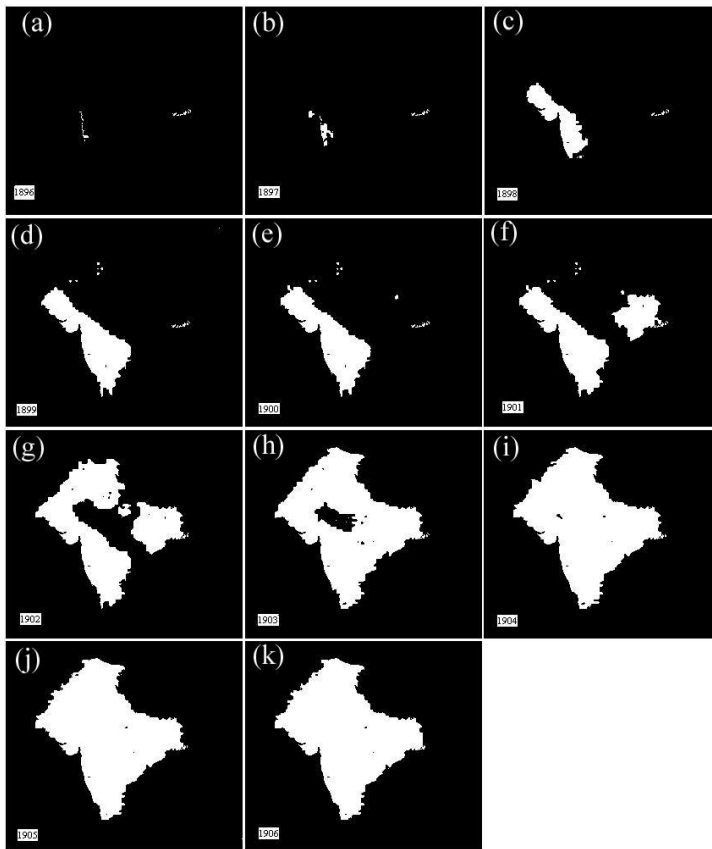


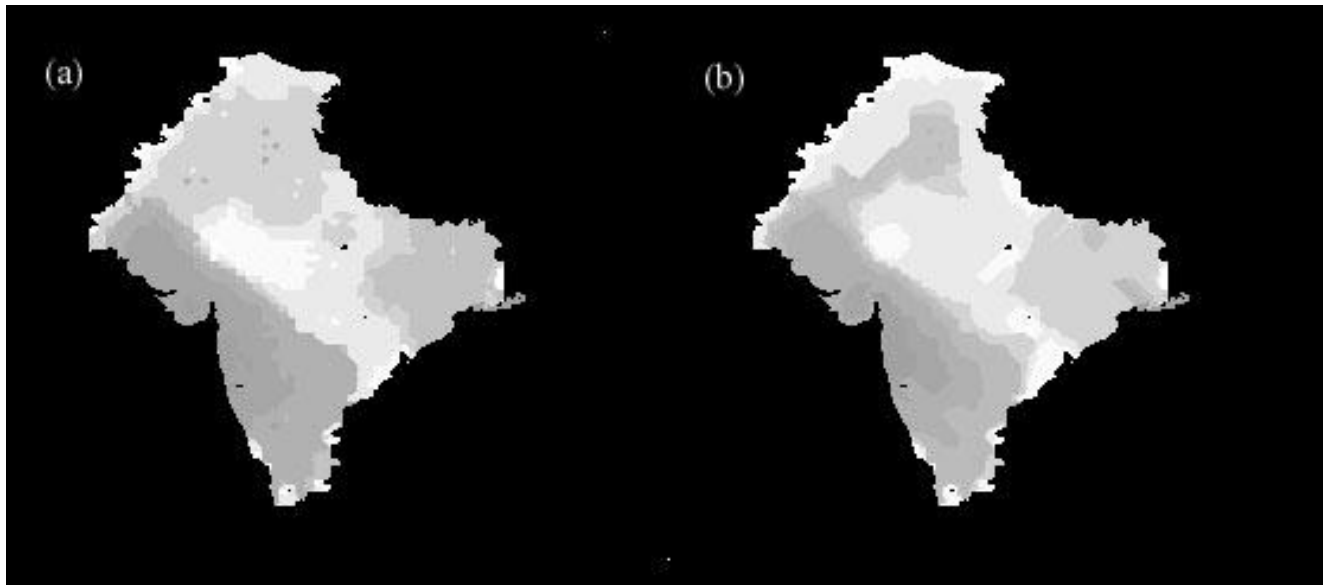
Fig. 4. A sequence of interpolated sets (slices) in between the two input slices shown in Figs. 3a, b. Equations 8(a) and 14 are used to recursively generate the interpolated slices. The layer depicting water bodies with magenta color is the median set shown in Fig. 3c.

Observed and Interpolated Epidemic Spread Maps

<http://www.isibang.ac.in/~bsdsagar/AnimationOfEpidemicSpread.avi>



Observed and Interpolated Sequences



III.II. Spatial Reasoning

Strategically important set(s)

Directional spatial relationship

Point-polygon conversion

III.II.I. Strategically significant state(s)

$$H/P(A_{ij}) = - \sum_{\substack{\forall j \\ i \rightarrow i}} \Pr \left[P(A_{ij}) \log \Pr \left[P(A_{ij}) \right] \right]$$

$$H/C(A_{ij}) = - \sum_{\substack{\forall j \\ i \neq j}} \Pr \left[C(A_{ij}) \log \Pr \left[C(A_{ij}) \right] \right]$$

$$H/d(A_{ij}) = - \sum_{\substack{\forall j \\ i \neq j}} \Pr \left[d(A_{ij}) \log \Pr \left[d(A_{ij}) \right] \right]$$

$$H/d(A_{ji}) = - \sum_{\substack{\forall i \\ i \neq j}} \Pr \left[d(A_{ji}) \log \Pr \left[d(A_{ji}) \right] \right]$$

$$(SH_i^P) = \min_{\forall i} \left\{ H / P(A_{ij}) \right\} \quad (SA_i^P) = \max_{\forall i} \left\{ \overline{\sum_i NP(A_{ij})} \right\}$$

$$(SH_i^d) = \min_{\forall i} \left\{ \min \left\{ H / d(A_{ij}), H / d(A_{ji}) \right\} \right\}$$

$$(SH_i^C) = \min_{\forall i} \left\{ H / C(A_{ij}) \right\}$$

$$(SA_i^d) = \min_{\forall i, j} \left\{ \min \left[\overline{\sum_i Nd(A_{ij})}, \overline{\sum_j Nd(A_{ji})} \right] \right\}$$

$$(SA_i^c) = \max_{\forall i} \left\{ \overline{\sum_i C(A_{ij})} \right\}$$

$$P(A_{ij}) = P \left[(A_i \oplus B) \cap (A_j) \right]$$

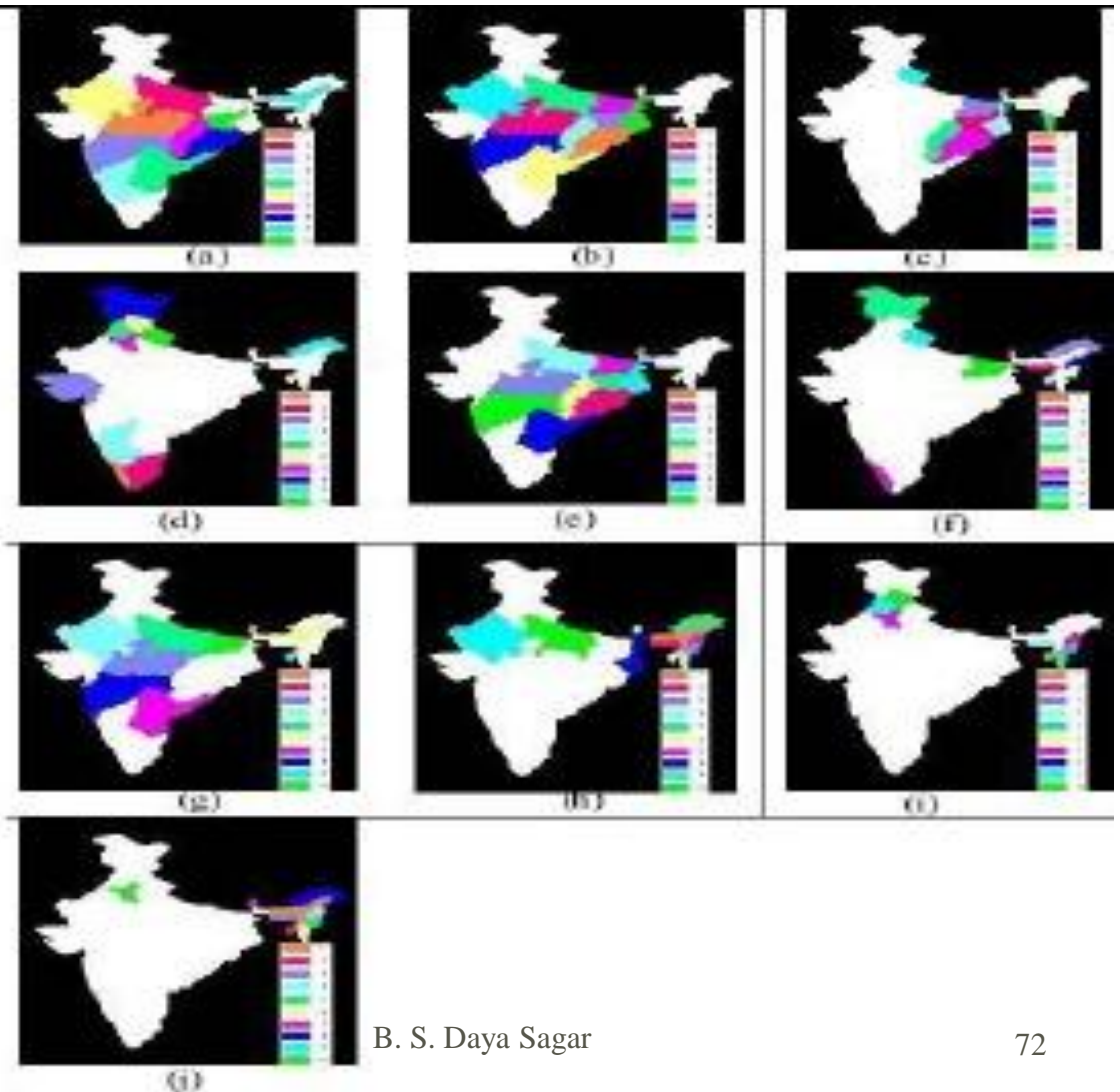
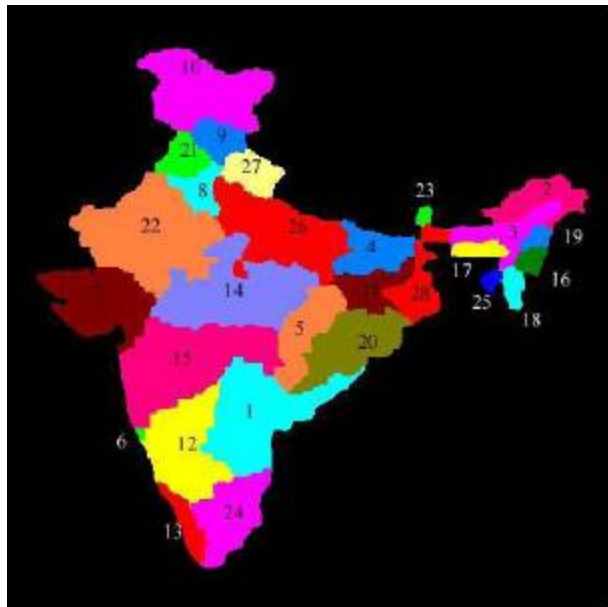
$$d(A_{ij}) = \min_{i \neq j} \left\{ n : A_j \subseteq (A_i \oplus nB) \right\},$$

$$C(A_{ij}) = C(A_{ji})$$

$$= \left[\frac{\rho(A_{ij})}{\max \left[d(A_{ij}), d(A_{ji}) \right]} \right]$$

$$= \left[\frac{\rho(Nd(A_{ij}))}{\max \left[Nd(A_{ij}), Nd(A_{ji}) \right]} \right]$$

Strategically significant state(s) w.r.t 10 parameters



III.II.II Directional Spatial Relationship

<http://www.isibang.ac.in/~bsdsagar/AnimationOfDirectionalSpatialRelationship.wmv>

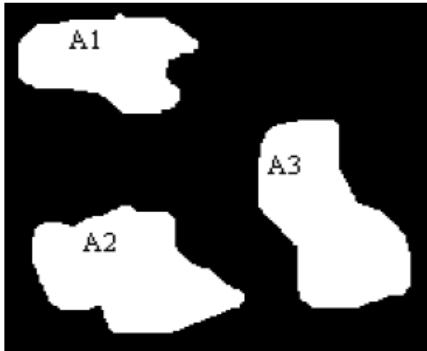


Fig. 1. (A₁, A₂, A₃) three disjoint objects possessing different directional spatial relationship.

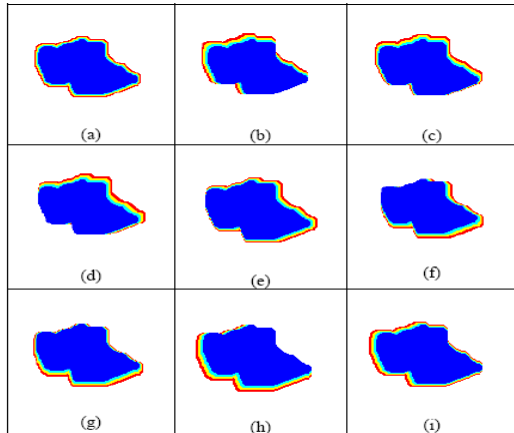


Fig. 5. Directional dilations on objects A by all nine origins. (a) $A \oplus B^0$, (b) $A \oplus B^1$, (c) $A \oplus B^2$, (d) $A \oplus B^3$, (e) $A \oplus B^4$, (f) $A \oplus B^5$, (g) $A \oplus B^6$, (h) $A \oplus B^7$, (i) $A \oplus B^8$.

1	1	1	(i)	1	1	1	(i)	1
1	(i)	1	1	1	1	1	1	1
1	1	1	1	1	1	1	1	1
(B^0)			(B^1)			(B^2)		
1	1	(i)	1	1	1	1	1	1
1	1	1	1	1	(i)	1	1	1
1	1	1	1	1	1	1	1	(i)
(B^3)			(B^4)			(B^5)		
1	1	1	1	1	1	1	1	1
1	1	1	1	1	1	(i)	1	1
1	(i)	1	(i)	1	1	1	1	1
(B^6)			(B^7)			(B^8)		

Fig. 3. Structuring element is shown with different possible origins. Except the first structuring element for which the origin is shown at the center, all other eight structuring elements are with other eight possible positions as origins. Those eight other structuring elements are asymmetric structuring elements as their transposes are not equivalents of their non-transposed versions.

$$\Delta(A_i, A_j) = i \left| \min_{\forall i} \left\{ n : A_j \subseteq \left(A_i \oplus n \hat{B}^i \right) \right\} \right|$$

TABLE 1. DISTANCES, UNIQUE ORIGINS AND DIRECTIONS

	Minimum Dilatation Distances			Unique Origins			Directional Relations			Visualization of Directional Relations					
	A ₁	A ₂	A ₃	A ₁	A ₂	A ₃	A ₁	A ₂	A ₃	A ₁	A ₂	A ₃			
A ₁	0	53	50	A ₁	0	2	1	A ₁	C	N	NW	A ₁			
A ₂	46	0	36	A ₂	6	0	7	A ₂	S	C	SW				
A ₃	52	49	0	A ₃	5	3	0	A ₃	SE	NE	C				

1	2	3	NW	N	NE			
8	0	4	W	C	E			
7	6	5	SW	S	SE			
(a)			(b)			(c)		

Fig. 4 Shows (a) origins of structuring element, and their corresponding directions in (b) and color codes in (c).

III.II.III Point-to-Polygon Conversion

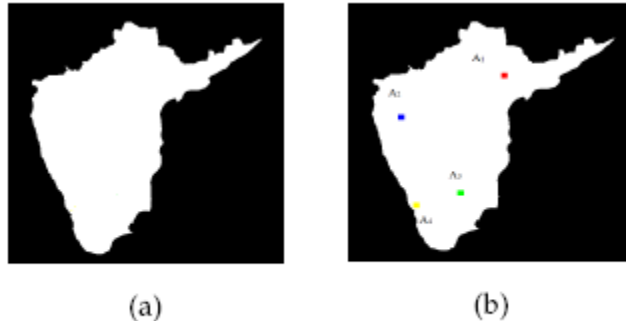


Fig. 2. (a) region considered is south India, and (b) gauge-station locations (A_1, A_2, A_3, A_4).

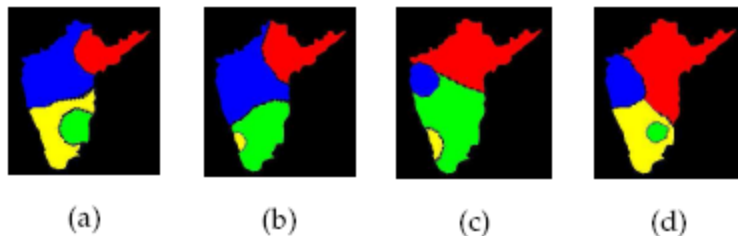


Fig. 3. The variable strengths (in terms of propagation speeds are given as (a) $A_2 > A_4 > A_1 > A_3$, (b) $A_2 > A_1 > A_3 > A_4$, (c) $A_1 > A_3 > A_2 > A_4$, and (d) $A_1 > A_4 > A_2 > A_3$.

$$Z(A_i) = \bigcup_n (\delta^{n_i}(A_i) \cap A) \setminus \bigcup_{\forall j} (\delta^{n_j}(A_j) \cap A)$$

$$Z(A) = \left(\bigcup_i (Z(A_i)) \right)^c$$

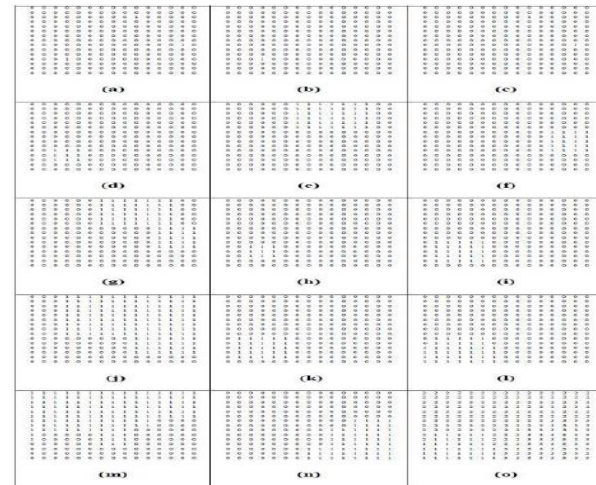


Fig. 51. (a) original map with three points (shown with 1s) for (A_1), (A_2), and (A_3). (b) i^{th} point (A_1)-(A_1). (c) union of i^{th} points. $\bigcup_i A_i = (A_1) \cup (A_2)$. (d) first cycle of dilation of i^{th} point by B (Square in shape) with the propagation speed of $\lambda=1$, denoted by $\sigma^1(A_1)$. (e) first cycle of dilation of i^{th} point (A_2) by B with the propagation speed of $\lambda=3$, $\sigma^3(A_2)$. (f) first cycle of dilation of i^{th} point (A_3) by B with the propagation speed of $\lambda=2$, $\sigma^2(A_3)$. (g) union of $\sigma^1(A_1)$ and $\sigma^2(A_3)$. (h) $\sigma^1(A_1) \setminus \sigma^2(A_3) \cup \sigma^3(A_2)$. (i) $\sigma^1(A_1)$. (j) similarly for next iteration: $\sigma^2(A_1) \cup \sigma^3(A_2)$. (k) $\sigma^2(A_1) \setminus \sigma^3(A_2) \cup \sigma^3(A_2)$. (l) $Z(A) = \bigcup_i [\sigma^{n_i}(A_i) \setminus \sigma^{n_j}(A_j) \cup \sigma^{n_i}(A_i)]$. (m) similarly follow the steps from (b-1) by changing the i^{th} point from (A_1) to (A_2), and by treating (A_1) and (A_2) as i^{th} points; the $Z(A_2)$ is obtained. (n) obtained $Z(A_1)$, and (o) three zones $Z(A_1)$, $Z(A_2)$, and $Z(A_3)$ are shown with 1s, 2s, and 3s.

Point-to-Polygon Conversion

<http://www.isibang.ac.in/~bsdsagar/AnimationOfPointPolygonConversion.wmv>

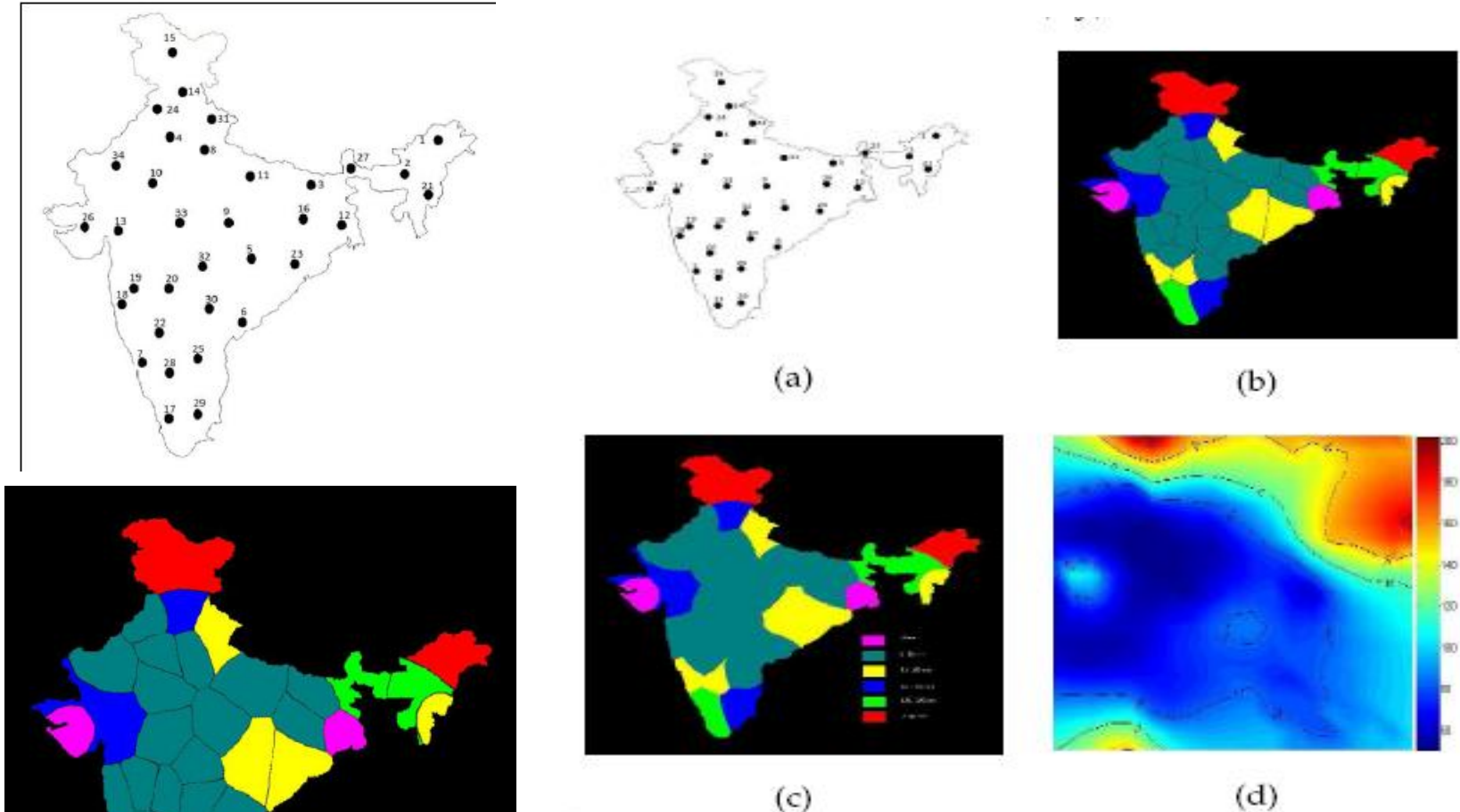


Fig. 4. (a) 34 points (locations) of rain-gauge stations spread over India indexed ($A_1 - A_{34}$), (b) Rainfall zonal map generated by having various possible propagation speeds, and the variable strengths in terms of propagation speeds are given according to ranks shown in Table 1, (c) broader zones obtained after merging the zones (Fig. 4b) obtained with similar propagation speeds, and (d) kriged map generated for 34 gauge station data.

ACKNOWLEDGEMENTS

I would like to gratefully acknowledge organizers of IAMG conference Robert Marschallinger, Fritz Zobl, IAMG President Vera Pawlowsky-Glahn, Vice President Qiuming Cheng, Treasurer Gina Ross for arranging all that I have asked to reach Salzburg. I am most grateful to Qiuming Cheng, Chairman of GML selection committee, Katsuaki Koike and Jean Serra, members of the GML selection committee for choosing me as 2011 Georges Matheron Lecturer of IAMG. Support given by Bimal Roy and Sankar Pal (Current and Former Directors of Indian Statistical Institute) who created a great environment for academic research is gratefully acknowledged.

Grateful to collaborators, mentors, reviewers, examiners, friends, employers, well-wishers, and doctoral students—S. V. L. N. Rao, B. S. P. Rao, M. Venu, K. S. R. Murthy, Gandhi, Srinivas, Radhakrishnan, Lea Tien Tay, Chockalingam, Lim Sin Liang, Teo Lay Lian, Dinesh, Jean Serra, Gabor Korvin, Arthur Cracknell, Deekshatulu, Philippos Pomonis, Peter Atkinson, Hien-Teik Chuah, Laurent Najman, Jean Cousty, Christian Lantuejoul, Christer Kiselman, Alan Tan, Sankar Pal, Bimal Roy, Lim Hock, VC Koo, Rajesh, Ashok, Pratap, Rajashekara, Saroj Meher, Alan Wilson, B. K. Sahu, K. V. Subbarao, Baldev Raj, C. Babu Rao, and several others.

From bottom of my heart, I express my gratitude to my wife Latha for her understanding, patience, and love. I feel relieved from stress when I listen to tales and stories that my children (Saketh and Sriniketh), learnt at school, narrate me.

Selected References

- ∞ Horton, R. E. (1945). Erosional development of stream and their drainage basin: hydrological approach to quantitative morphology, Bulletin of the Geophysical Society of America, 56, pp. 275-370.
- ∞ Langbein, W. B. (1947). Topographic characteristics of drainage basins, U.S. Geological Survey Professional Paper. 968-C, pp. 125-157.
- ∞ Strahler, A. N. (1952). Hypsometric (area-altitude) analysis of erosional topography: Bulletin Geological Society of America, v. 63, no. II, pp. 1117-1141.
- ∞ Strahler, A. N. (1957). Quantitative analysis of watershed geomorphology. EOS Transactions of the American Geophysical Union, 38(6):913-920.
- ∞ Strahler, A. N. (1964). Quantitative geomorphology of drainage basins and channel networks, In Handbook of applied Hydrology (ed. V. T. Chow), New York, McGraw Hill Book Co., Section 4, pp. 4-39 - 4-76.
- ∞ Barbera, P. L. and Rosso, R. (1989). On the fractal dimension of stream networks, Water Resources Research, 25(4):735-741.
- ∞ Tarboton, D. G., Bras, R. L. and Rodríguez-Iturbe, I. (1990). Comment on “On the fractal dimension of stream networks” by Paolo La Barbera and Renzo Rosso. Water Resources Research, 26(9):2243-4.
- ∞ Maritan, A., Cololairi, F., Flammini, A., Cieplak, M., and Banavar, J. R. (1996). Universality classes of optimal channel networks. Science, 272, 984.
- ∞ Maritan, A., Rigon, J. R. Banavar, and A. Rinaldo (2002). Network allometry, Geophysical Research Letters, 29(11), p. 1508-1511.
- ∞ Rodríguez-Iturbe, I. and Rinaldo, A. (1997). Fractal River Basins: Chance and Self-organization, Cambridge University Press, Cambridge.
- ∞ Mandelbrot, B. B. (1982). The Fractal Geometry of Nature. Freeman, San Francisco.
- ∞ Turcotte, D. L. (1997). Fractals in Geology and Geophysics, Cambridge University Press, Cambridge.
- ∞ Matheron, G. (1975). Random Sets and Integral Geometry, John Wiley Hoboken, New Jersey.
- ∞ Serra, J. (1982), Image Analysis and Mathematical Morphology, Academic Press, London.
- ∞ Peucker, T. K. and Douglas, D. H. (1975). Detection of surface-specific points by local parallel processing of discrete terrain elevation data, Computer Vision, Graphics and Image Processing, 4, p. 375-387.
- ∞ Veitzer, S. A. and Gupta, V. K., (2000). Random self-similar river networks and derivations of generalized Horton laws in terms of statistical simple scaling, Water Resources Research, Volume 36 (4), 1033-1048.

Selected References

- ✎ SAGAR, B. S. D.; VENU, M.; SRINIVAS, D. (2000): Morphological operators to extract channel networks from digital elevation models”, *International Journal of Remote Sensing*, VOL. 21, 21-30.
- ✎ SAGAR, B. S. D.; MURTHY, M. B. R.; RAO, C. B.; RAJ, B. (2003): Morphological approach to extract ridge-valley connectivity networks from digital elevation models (DEMs), *International Journal of Remote Sensing*, VOL. 24, 573 – 581.
- ✎ TAY, L. T.; SAGAR, B. S. D.; CHUAH, H. T. (2005): Analysis of geophysical networks derived from multiscale digital elevation models: a morphological approach, *IEEE Geoscience and Remote Sensing Letters*, VOL. 2, 399-403.
- ✎ LIM, S. L.; KOO, V. C.; SAGAR, B. S. D. (2009): Computation of complexity measures of morphologically significant zones decomposed from binary fractal sets via multiscale convexity analysis, *Chaos, Solitons & Fractals*, VOL. 41, 1253–1262.
- ✎ LIM, S. L.; SAGAR, B. S. D. (2007): Cloud field segmentation via multiscale convexity analysis, *Journal Geophysical Research-Atmospheres*, VOL. 113, D13208, doi:10.1029/2007JD009369.
- ✎ SAGAR, B. S. D. (1996): Fractal relations of a morphological skeleton, *Chaos, Solitons & Fractals*, VOL. 7, 1871-1879.
- ✎ SAGAR, B. S. D.; TIEN, T. L. (2004): Allometric power-law relationships in a Hortonian Fractal DEM, *Geophysical Research Letters*, VOL. 31, L06501.
- ✎ TAY, L. T.; SAGAR, B. S. D.; CHUAH, H. T. (2006): Allometric relationships between travel-time channel networks, convex hulls, and convexity measures, *Water Resources Research*, VOL. 46, W06502.
- ✎ SAGAR, B. S. D. (2007): Universal scaling laws in surface water bodies and their zones of influence, *Water Resources Research*, VOL. 43, W02416.
- ✎ SAGAR, B. S. D.; CHOCKALINGAM, L. (2004): Fractal dimension of non-network space of a catchment basin, *Geophysical Research Letters*, VOL. 31, L12502.
- ✎ CHOCKALINGAM, L.; SAGAR, B. S. D. (2005): Morphometry of networks and non-network spaces, *Journal of Geophysical Research*, VOL. 110, B08203.
- ✎ TAY, L. T.; SAGAR, B. S. D.; CHUAH, H. T. (2007): Granulometric analysis of basin-wise DEMs: a comparative study, *International Journal of Remote Sensing*, VOL. 28, 3363-3378.
- ✎ SAGAR, B. S. D.; SRINIVAS, D.; RAO, B. S. P. (2001): Fractal skeletal based channel networks in a triangular initiator basin, *Fractals*, VOL. 9, 429-437.
- ✎ SAGAR, B. S. D.; VENU, M.; GANDHI, G.; SRINIVAS, D. (1998): Morphological description and interrelationship between form and structure: a scope to geomorphic evolution process modelling, *International Journal of Remote Sensing*, VOL. 19, 1341-1358.

Selected References

- ✎ SAGAR, B. S. D. (2005): Discrete simulations of spatio-temporal dynamics of small water bodies under varied streamflow discharges, *Nonlinear Processes in Geophysics*, VOL. 12, 31-40, 2005.
- ✎ SAGAR, B. S. D. (2010): Visualization of spatiotemporal behavior of discrete maps via generation of recursive median elements, *IEEE Transactions on Pattern Analysis and Machine Intelligence*, VOL. 32, 378-384.
- ✎ RAJASHEKHARA, H. M.; PRATAP VARDHAN; SAGAR, B. S. D. (2011): Generation of Zonal Map from Point Data via Weighted Skeletonization by Influence Zone, *IEEE Geoscience and Remote Sensing Letters* (Revised version under review).
- ✎ SAGAR, B. S. D.; PRATAP VARDHAN; DE, D. (2011): Recognition and visualization of strategically significant spatial sets via morphological analysis, *Computers in Environment and Urban Systems*, (Revised version under review).
- ✎ PRATAP VARDHAN; SAGAR, B. S. D. (2011): Determining directional spatial relationship via origin-specific dilation-distances, *IEEE Transactions on Geoscience and Remote Sensing* (Under Review).

Thank You

Q & A